# Coordination of rooting, xylem, and stomatal strategies explains the response of conifer forest stands to multi-year drought in the Southern Sierra Nevada of California

Junyan Ding[1,2], Polly Buotte[3], Roger Bales[4], Bradley Christoffersen[5], Rosie A. Fisher[6,7], Michael Goulden[8], Ryan Knox[1], Lara Kueppers[1,3], Jacquelyn Shuman[6], Chonggang Xu[9], Charles D. Koven[1]

1. Climate and Ecosystem Sciences Division, Lawrence Berkeley National Lab, Berkeley, USA
2. Pacific Northwest National Lab, Richland, WA, USA
3. Energy and Resources Group, University of California, Berkeley, USA
4. Sierra Nevada Research Institute, University of California, Merced, USA
5. Department of Biology, University of Texas, Rio Grande Valley, USA
6. Climate and Global Dynamics Division, National Center for Atmospheric Research, Bold, USA
7. Laboratoire Évolution & Diversité Biologique, CNRS:UMR 5174, Université Paul Sabatier, Toulouse, France
8. Dept. of Earth System Science, University of California, Irvine, USA
9. Earth and Environmental Sciences Division, Los Alamos National Laboratory, Santa Fe, New Mexico, USA

Corresponding author: Junyan Ding (junyan.ding@pnnl.gov)

Key Points:

- We perform a sensitivity analysis using the model FATES-Hydro to explore the coordination of leaf, xylem, and root hydraulic traits of pine in the Southern Sierra Nevada.
- We find that rooting depth is the major control on water and carbon fluxes and that deep-rooted pines with risky stomata have the highest GPP but also the highest drought mortality risk.
- Resolving both plant water sourcing strategies and subsurface processes is critical to representing drought impacts on conifer forests.

## Abstract

Extreme droughts are a major determinant of ecosystem disturbance, which impacts plant communities and feeds back into climate change through changes in plant functioning. However, the complex relationships between above- and below-ground plant hydraulic traits and their role in governing plant responses to drought are not fully understood. In this study, we use a plant hydraulic model, FATES-Hydro, to investigate ecosystem responses to the 2012–2015 California drought in comparison with observations at a site in the southern Sierra Nevada that experienced widespread tree mortality during this drought.

We conduct a sensitivity analysis to explore how different plant water sourcing and hydraulic strategies lead to differential responses during normal and drought conditions.

The analysis shows that:

1. Deep roots that sustain productivity through the dry season are needed for the model to capture observed seasonal cycles of ET and GPP in normal years, and deep-rooted strategies are nonetheless subject to large reductions in ET and GPP when the deep soil reservoir is depleted during extreme droughts, in agreement with observations.
2. Risky stomatal strategies lead to greater productivity during normal years as compared to safer stomatal control, but they also lead to a high risk of xylem embolism during the 2012–2015 drought.
3. For a given stand density, stomatal and xylem traits have a stronger impact on plant water status than on ecosystem-level fluxes.

Our study highlights the significance of resolving plant water sourcing strategies to represent drought impacts on plants and consequent feedbacks in models.

## 1. Introduction

Understanding plant water use strategies and the resulting ecohydrologic processes in forests is critical for predicting surface water and energy exchange, carbon dynamics, and vegetation dynamics of water-constrained ecosystems in a changing climate. Mediterranean-type climates, as in California, are characterized by dry and hot summers and cool, wet winters, resulting in asynchronous supplies of energy and water. In addition to these climatic stresses, plants in California are further subject to high inter-annual variability in precipitation and periodic severe drought events, such as the recent 2012–2015 drought, which led to widespread tree mortality (Fettig et al. 2019). Together, these two climatic constraints present a unique challenge to the success of forests in California, which is likely to be exacerbated by a warming climate.

On evolutionary timescales, natural selection has led to a wide array of strategies and functional traits that allow plants to both grow and survive under a range of environmental conditions (Grime 1977, 1979; Coley et al. 1985; Westoby et al. 2002; Craine 2002; Reich et al. 2003). Given the centrality of water sourcing to plant physiology, plant hydraulic traits play an important role in water-constrained ecosystems. Once absorbed by fine roots, water flows through the vascular system via coarse roots, stems, and branches to leaves, where it evaporates through stomata. The rate of water flow through stems, and thus the supply to leaves, is determined by the hydraulic conductivity along this pathway. If the water potential of xylem tissue becomes too low, cavitation can occur and cause a loss of conductivity. Because this cavitation can damage the xylem network, trees have developed different strategies to mitigate this effect, all of which come at some cost. These strategies include 1) early stomatal closure or leaf deciduousness to reduce the flow of water at the cost of reduced carbon intake; 2) building cavitation-resistant xylem at the cost of increased hydraulic resistance; and 3) growing deep roots to access more moisture at the cost of higher carbon investment. In this study, we focus on the potential hydraulic strategies that trees in Californian ecosystems use, with a particular emphasis on how the coordination of hydraulic functional traits at the leaf, stem, and root levels is critical to carbon assimilation, transpiration, and consequently, the productivity and response of trees to drought (Matheny, Mirfenderesgi, and Bohrer 2017; Matheny et al. 2017; Mursinna et al. 2018a).

The traits that regulate stomatal conductivity are the most important hydraulic traits of leaves and the primary ones through which photosynthesis and transpiration are coupled. Stomatal behavior falls along a gradient between two extremes: stomata may close early during water stress to avoid the risk of hydraulic failure or remain open to maximize carbon uptake while exposing xylem to a higher risk of embolism (Martínez-Vilalta, Sala, and Piñol, 2004; McDowell et al., 2008; Skelton, West, & Dawson, 2015; Matheny et al., 2017). The sensitivity of stomata to water stress determines where the stomata operate along the safety-risk gradient and thus the degree to which carbon intake is traded for preventing the cavitation of xylem. Where the best stomatal strategy sits along the safety-risk gradient would depend on the physical environment.

Maximum hydraulic conductivity and vulnerability to cavitation are the two key xylem hydraulic traits. Differences in the anatomy and morphology of the conductive xylem cell structure and anatomy (Hacke et al. 2017) lead to differences in maximum conductivity and the water potential at which cavitation starts to occur (Pockman & Sperry, 2000; Sperry 2003). Within the conifers, there are at least three mechanisms that lead to a tradeoff between xylem safety and efficiency. The first is the morphology of the xylem conduit. It is widely acknowledged that narrow (or short) tracheid are safer than wider (or longer) tracheid but have lower conductance per sap area (Choat and Pittermann 2009). Second are the intervessel pit membranes. Thicker and less porous membranes prevent the spread of air but increase the hydraulic resistance of xylem (e.g., Li et al., 2016; Pratt & Jacobsen, 2017). The third mechanism comes from the division of limited space (Pratt and Jacobsen 2017). With the same cross-sectional area of conduits, vessels with a thicker cell wall provide stronger mechanical support, so that the conduits are less likely to collapse when xylem water potential becomes more negative; however, this reduces the area that can be used for conduits transporting water. While these physiological constraints require that the tradeoff exists to some extent, in many studies, this tradeoff appears to be weak, and there are certainly species that have both safe and efficient xylem. Further, there are many other plant traits that can affect safety, such as wood density (Pratt and Jacobsen 2017), pit anatomy (Sperry & Hacke 2004, Lens et al. 2011), and biochemistry (Gortan et al. 2011). These traits can have large variations among different plant types. The tradeoff will be weakened when grouping plants at a coarse scale, e.g., by biomass, families, and/or across a range of geological and climatic regions. But when focusing on certain

species in a particular region, the tradeoff becomes stronger, as demonstrated by many local studies (e.g., Barnard et al. 2011, Corcuera et al. 2011, Baker et al. 2019). For example, Kilgore et al. (2021) show that there is a clear safety-efficiency tradeoff across pine trees in a specific location in the western US. Thus, while we acknowledge that there are many exceptions to the xylem safety-efficiency tradeoff, it is a useful framework for examining plant strategies for dealing with drought.

The traits that govern the hydraulic function of plant root systems are also critically important, but they are the least understood, studied, and quantified. These traits include the rooting depth, the root-to-shoot ratio, the vertical and lateral distribution of roots, and the fine root density and diameter, all of which are related to water uptake (Canadell et al., 2007; Allen, 2009; Reichstein et al., 2014; Wullschleger et al., 2014). In general, species with deeper roots can access water at greater depths, which is unavailable to more shallowly rooted species (Jackson et al., 1996; Canadell et al., 1996). The vertical root distribution can affect the water uptake and thus the evapotranspiration (ET) pattern during the dry-down period (Teuling, Uijlenhoet, and Troch 2006). This in turn affects the seasonal distribution of water over the soil depth and thereby the resilience of plants to seasonal droughts (Yu, Zhuang, and Nakayamma 2007). The vertical root distribution is also a means of belowground niche differentiation (Ivanov et al. 2012; Kulmatiski and Beard 2013), whereas the extent of the lateral root distribution dictates the competition for water (Agee et al. 2021). Whether a plant can benefit from having deep roots is related to the plant's leaf and xylem hydraulic traits (e.g., Johnson et al. 2018, Mackay et al. 2020), thus requiring coordination of rooting and hydraulic traits.

Given the strength of the Mediterranean-type climate of California, the coordination of rooting and hydraulic strategies will play a critical role in forest dynamics. However, the interplay of rooting and hydraulic strategies and their impact on ecosystem processes haven't been well understood. In this study, we address this question at the Soaproot site (CZ2) of the southern Sierra Nevada of California as the study area. The CZ2 site was strongly affected by the 2012–2015 drought, with extremely high tree mortality rates (90% of the pine died) (Fettig et al. 2019). While the 2012–2015 drought was widespread across California, the highest rates of tree mortality occurred in the southern Sierra Nevada, centered around an elevation similar to this site (1160 m to 2015 m, Asner et al. 2016, Goulden and Bales 2019). This mid-elevation region is

149 also characterized by the highest forest productivity along an elevation gradient from foothill
150 woodlands to subalpine forest (Kelly and Goulden 2016). This leads us to ask whether strategies
151 associated with high productivity have exposed trees to a high mortality risk under prolonged
152 drought.

153 Specifically, here we use the Functionally Assembled Terrestrial Ecosystem Simulator, in
154 a configuration that includes plant hydraulics (FATES-Hydro), to explore the tradeoffs
155 associated with differing hydraulic strategies and, in particular, their implications for plant
156 productivity and the risk of drought-induced mortality. We conduct a sensitivity analysis using
157 FATES-Hydro in comparison with observations from the CZ2 eddy covariance site to investigate
158 how stomatal, xylem, and rooting strategies affect the ecosystem and physiologic processes of
159 the forest and whether that may explain the high rates of both productivity and drought-
160 associated mortality of conifers at CZ2. We note that this is not an exhaustive model parameter
161 sensitivity study. The main purpose is to use a sensitivity analysis to explore scientific questions
162 around hydraulic trait tradeoffs.

163 **2. Methods**

164 2.1 Study site

165 The Soaproot site is a 543-ha headwater catchment at 1100m elevation (37°2.4' N,
166 119°15.42' W), which is at the lower boundary of the rain–snow transition line with warm, dry
167 summers and cool, wet winters (Geen et al. 2018). The mean annual temperature is about 13.8°C
168 (Goulden et al., 2012). Under normal conditions, the annual precipitation is about 1300 mm, but
169 during a dry year, the precipitation can drop to 300-600mm. (Bales et al. 2018). The site is a
170 ponderosa pine (*Pinus ponderosa*) dominated conifer ecosystem exhibiting high productivity
171 (Kelly and Goulden (2016) reported 2.1 tC/ha/year average annual gross stem wood production
172 averaged). Other species include California black oak (*Quercus kelloggii* Newberry), and incense
173 cedar (*Calocedrus decurrens*).

174 Soils at the Soaproot site are mainly of the Holland (fine-loamy, mesic Ultic Haploxeralfs)
175 and Chaix (coarse-loamy, mesic Typic Dystroxerepts) series, which are representative of soils
176 across a similar elevation band of the western Sierra Nevada (Mooney and Zavaleta 2003). Soils
177 of the Holland series have sandy loam surface texture and underlying Bt horizons with sandy

clay loam textures, while soils of the Chaix series have sandy loam textures throughout the profile. The regolith depth is estimated to be 15m (Holbrook et al., 2014). The total porosity over the whole regolith depth of the site is estimated to be 1620 mm and the total available storage porosity (plant accessible water storage capacity), which is the difference in volumetric water content between field capacity and permanent wilting point (~ -6Mpa) to be 1400 mm (Klos et al. 2017). The available water storage capacity is approximately 0.20 $cm^3\ cm^{-3}$ in the upper regolith (0–5 m depth) which decreases to 0.05 $cm^3\ cm^{-3}$ or less in the lower regolith (below 5 m depth) (Holbrook et al., 2014).

An eddy-covariance flux tower was installed at this site in September 2010. The elevation of the tower is 1160 m above sea level. Instruments on the flux tower track changes in carbon dioxide, water vapor, air temperature, relative humidity, and other atmospheric properties. We compare the simulated gross primary productivity (GPP) and latent heat flux with the flux tower measurements over the period from 2011 to 2015 (Goulden and Bales 2019). We computed the Root Mean Square Error (RMSE) of the hourly mean diurnal cycle of each month. This allows us to examine the capacity of FATES-Hydro to predict the carbon and water fluxes. The transpiration at the site contributed to the majority of the ET as indicated by the measurements from an adjacent catchment, as well as the fact that the site is fully vegetated with an annual LAI around 3 to 4.

## 2.2 FATES-Hydro model and parameterization

### 2.2.1 The FATES-Hydro model

FATES is a cohort-based, size- and age-structured dynamic vegetation model, where long-term plant growth and mortality rates and plant competition emerge as a consequence of physiological processes. In the model, multiple cohorts grow on the same land unit, share the soil water, and interact with each other through light competition. FATES is coupled within both the CLM5 (Lawrence et al., 2019) and the ELM (Golaz et al., 2020) land surface models (LSMs). In this study, FATES is coupled with the CLM5. FATES-Hydro is a recent development of the FATES model (Fisher et al., 2015; Koven et al., 2020), in which a plant hydro-dynamic module, originally developed by Christoffersen et al. (2016), is coupled to the existing photosynthesis and

soil hydraulic modules. FATES-Hydro is described in more detail by Xu et al., (in review, https://doi.org/10.5194/egusphere-2023-278 ) and its supplementary material.

Conceptually, plant hydraulic models can be broadly grouped into two types. The first group represents the plant hydraulic system as analogous to an electrical circuit (e.g. Mackay et al. 2011, Huang et al. 2017, Eller et al. 2018, Kennedy et al. 2019). The total resistance of the plant is calculated from the resistance of each compartment using Ohm's law. There is no storage of water in the plants and the transpiration from plants at any given time step is considered to come directly from soil storage. The second group represents plant hydraulics by a series of connected porous media, corresponding to each plant compartment (e.g. Bohrer et al. 2005, Janott et al. 2011, Xu et al., 2016, Christoffersen et al., 2016). The porous media model takes into account the water storage in the plant. The flow between two adjacent compartments is driven by the difference in the water potential, mediated by the hydraulic conductivity. FATES-Hydro falls in the second group. The various models in the second group differ in the exact formulas used to describe the pressure-volume and pressure-conductivity relations, as well as different numbers and arrangement of nodes within the soil-plant-atmosphere system.

In FATES-Hydro, for each plant cohort, the hydraulic module tracks water flow along a soil–plant–atmosphere continuum of a representative individual tree based on hydraulic laws, and updates the water content and potential of leaves, stem, and roots with a 30 minute model time step. Water flow from each soil layer within the root zone into the plant root system is calculated as a function of the hydraulic conductivity as determined by root biomass and root traits such as specific root length, and the difference in water potential between the absorbing roots and the rhizosphere. The vertical root distribution is based on Zeng's (2001) two parameter power law function, which takes into account the regolith depth:

$$Y_i = \frac{0.5(e^{-r_a z_{li}} + e^{-r_b z_{li}}) - 0.5(e^{-r_a z_{ui}} + e^{-r_b z_{ui}})}{1 - 0.5(e^{-r_a z} + e^{-r_b z})}, \qquad \text{(Eq 1)}$$

where $Y_i$ is the fraction of fine or coarse roots in the $i$th soil layer, $r_a$ and $r_b$ are the two parameters that determine the vertical root distribution, $Z_{li}$ is the depth of the lower boundary of the $i$th soil layer, and $Z_{ui}$ is the depth of the upper boundary of the $i$th soil layer, and $Z$ is the total

regolith depth. The vertical root distribution affects water uptake by the hydrodynamic model by distributing the total amount of root, and thus root resistance, through the soils.

The total transpiration of a tree is the product of total leaf area (LA) and the transpiration rate per unit leaf area (J). In this version of FATES-Hydro, we adopt the model developed by Vesala et al. (2017) to take into account the effect of leaf water potential on the within-leaf relative humidity and transpiration rate:

$$E = LA \cdot J \quad \text{(Eq 2a)}$$

$$J = \rho_{atm} \frac{(q_l - q_s)}{1/g_s + r_b} \quad \text{(Eq 2b)}$$

$$q_l = \exp\left(\frac{w \cdot LWP \cdot V_{H2O}}{R \cdot T}\right) \cdot q_{sat} \quad \text{(Eq 2c)}$$

where E is the total transpiration of a tree, LA is the total leaf area ($m^2$), J is the transpiration per unit leaf area (kg $s^{-1}$ $m^{-2}$), $\rho_{atm}$ is the density of atmospheric air (kg $m^{-3}$), $q_l$ is the within-leaf specific humidity(kg $kg^{-1}$), $q_s$ is the atmosphere specific humidity (kg $kg^{-1}$), $g_s$ is the stomatal conductance per leaf area, $r_b$ is the leaf boundary layer resistance(s $m^{-1}$), *w* is a scaling coefficient (unitless), which can vary between 1 and 7, and here we use a value of 3; LWP is the leaf water potential (Mpa), $V_{H2O}$ is the molar volume of water ($18 \times 10^{-6}$ $m^3$ $mol^{-1}$), *R* is the universal gas constant, and T is the leaf temperature (K).

The sap flow from absorbing roots to the canopy through each compartment of the tree along the flow pathway (absorbing roots, transport roots, stem, and leaf) is computed according to Darcy's law in terms of the plant sapwood water conductance, the water potential gradient:

$$Q_i = -K_i[\rho_w g(z_i - z_{i+1}) + (\Psi_i - \Psi_{i+1})] \quad \text{(Eq 3)}$$

where $\rho_w$ is the density of water; $z_i$ is the height of the compartment(m); $z_{i+1}$ is the height of the next compartment down the flow path (m); $\Psi_i$ is the water potential of the

compartment(Mpa); $\Psi_{i+1}$ is the water potential of the next compartment down the flow path(Mpa); and $K_i$ is the hydraulic conductivity of the compartment (kg Mpa$^{-1}$ m$^{-1}$ s$^{-1}$). The hydraulic conductivity of the compartments is by the water potential and maximum hydraulic conductivity of the compartment through the pressure-volume (P-V) curve and the vulnerability curve (Manzoni et al. 2013, Christoffersen et al. 2016).

The plant hydrodynamic representation and numerical solver scheme within FATES-HYDRO follows Christoffersen et al. (2016). We made a few modifications to accommodate the multiple soil layers and to improve the numerical stability. First, to accommodate the multiple soil layers, we have sequentially solved the Richards' equation for each individual soil layer, with each layer-specific solution proportional to each layer's contribution to the total root-soil conductance. Second, to improve the numerical stability, we have an option to linearly extrapolate the PV curve beyond the residual and saturated tissue water content to avoid the rare cases of overshooting in the numerical scheme under very dry or wet conditions. Third, Christoffersen et al. (2016) use three phases to describe the PV curves: 1) dehydration phases representing capillary water (sapwood only), 2) elastic cell drainage (positive turgor), and 3) continued drainage after cells have lost turgor. Due to the possible discontinuity of the curve between these three phases, it leads to the potential for numerical instability. To resolve this instability, FATES-HYDRO added the Van Genuchten model (Van Genuchten 1980, July and Horton 2004) and the Campbell model (Campbell 1974) as alternatives to describe the PV curves.

In this study, we use the Van Genuchten model because of two advantages: 1) it is simple, with only three parameters needed for both curves, and 2) it is mechanistically based, with both the P-V curve and vulnerability curve derived from a pipe model, and thus connected through three shared parameters:

$$\Psi = \frac{1}{-\alpha} \cdot \left( \frac{1}{Se^{1/m}} - 1 \right)^{1/n} \qquad \text{(Eq 4a)}$$

$$FMC = \left( 1 - \left( \frac{(-\alpha \cdot \Psi)^n}{1 + (-\alpha \cdot \Psi)^n} \right)^m \right)^2 \qquad \text{(Eq 4b)}$$

where $\Psi$ is the water potential of the media (xylem in this case) (Mpa); $FMC$ is the fraction of xylem conductivity, $K/K_{max}$, (unitless); $\alpha$ is a scaling parameter for air entry point ($Mpa^{-1}$), $Se$ is the dimensionless standardized relative water content expressed as $Se=(\theta-\theta_r)/(\theta_{sat}-\theta_r)$ with $\theta$, $\theta_r$, $\theta_{sat}$ are volumetric water content ($m^3\ m^{-3}$), residual volumetric water content, and saturated volumetric water content correspondingly; and *m* and *n* are dimensionless (xylem conduits) size distribution parameters. The model assumes that xylem conductance can be restored as xylem water content increases due to increased water availability after a dry period without any hysteresis in the FMC curve.

The stomatal conductance is modelled in the form of the Ball-Berry conductance model (Ball et al. 1987, Oleson et al. 2013, Fisher et al. 2015):

$$g_s = b_{slp}\frac{A_n}{c_s / P_{atm}}\frac{e_s}{e_i} + b_{opt}\beta_t \quad \text{(Eq 5)}$$

where $b_{slp}$ and $b_{opt}$ are parameters that represent the slope and intercept in the Ball-Berry model, correspondingly. These terms are plant strategy dependent and can vary widely with plant functional types (Medlyn et al. 2011). The parameter $b_{opt}$ is also scaled by the water stress index $\beta_t$. $A_n$ is the net carbon assimilation rate ($\mu mol\ CO2\ m^{-2}\ s^{-1}$) based on Farquhar's (1980) formula. This term is also constrained by water stress index $\beta_t$ in the way that the $V_{cmax,25}$ is scaled by $\beta_t$ as $V_{cmax,25}\beta_t$ (Fisher et al. 2018). $c_s$ is the $CO_2$ partial pressure at the leaf surface (Pa), $e_s$ is the vapor pressure at the leaf surface (Pa), $e_i$ is the saturation vapor pressure (Pa) inside the leaf at a given vegetation temperature when $A_n = 0$.

The water stress index $\beta_t$, a proxy for stomatal closure in response to desiccation, is determined by the leaf water potential adopted from the $FMC_{gs}$ term from Christoffersen et al. (2016):

$$\beta_t = \left[ 1 + \left(\frac{\Psi_l}{P50_{gs}}\right)^{ags} \right]^{-1} \quad \text{(Eq 6)}$$

where $\Psi_l$ is the leaf water potential (MPa), $P50_{gs}$ is the leaf water potential of 50% stomatal closure, and $a_{gs}$ governs the steepness of the function. For a given value of $a_{gs}$, the $P50_{gs}$ controls the degree of the risk of xylem embolism (Christoffersen et al. 2016, Powell et al. 2017). A more negative $P50_{gs}$ means that, during leaf dry down from full turgor, the stomatal aperture stays open and thus allows the transpiration rate to remain high and xylem to dry out, which thus can maintain high photosynthetic rates, at the risk of exposing xylem to embolism and thus plant mortality. Conversely, a plant with a less negative $P50_{gs}$ will close its stomata quickly during leaf dry down, thus limiting transpiration and the risk of xylem embolism and mortality associated with it, at the cost of reduced photosynthesis.

2.2.2 Sensitivity analysis and parameterization

The goal of this analysis is to better understand how coordinated aboveground and belowground hydraulic traits determine plant physiological dynamics and the interplay between ecosystem fluxes and tissue moisture during the extreme 2012-2015 drought at the Soaproot site. We thus conduct a global sensitivity analysis on selected hydraulic parameters to explore the linkages of aboveground and belowground hydraulic strategies. We use a full-factorial design for the parameter sensitivity analysis in order to best investigate the relationships between parameters. Because this design requires a relatively small set of parameters or groups of parameters to vary, we chose parameters that represent the major axes of relatively well-understood stomatal, xylem and rooting mechanisms/strategies that control the hydraulic functioning of trees. We set the values of these parameters within the realistic (allowable biological) range based on online database, and literatures where the species and physical environment are as close to our system as possible. We list other major parameters and their estimates that are not varied in the sensitivity analysis (table 2). We acknowledge that the biggest disadvantage of this study is the lack of sufficient field data to constrain the model. This is a result of using a natural drought as an experiment of opportunity, which, because it was not

anticipated, did not allow for coordinated planning as would be the case in an experimentally-manipulated drought. The trees at that site had all died by the time we started this study.

The parameters that we vary here are 1) the pair of $r_a$ and $r_b$, which control vertical root distribution as deep vs shallow roots, 2) two sets of xylem parameters ($P_{50x}$, $K_{max}$, $m$, $n$, and $\alpha$) that jointly represent two distinct xylem strategies: efficient/unsafe and inefficient/safe xylem within the range observed for temperate conifer trees, and 3) the stomatal parameter $P50_{gs}$, which represents the stomatal strategy along a risky to safe gradient (Table 1). The ranges of root parameters are chosen so that the effective rooting depth, above which 95% of root biomass stays, varies from 1m to 8m which is the possible range at the Soaproot site, as indicated by current knowledge of the subsurface structure (see Klos et al., 2017). Note, here we refer to a higher proportion of roots in deep subsurface layers as 'deep rooting' (e.g effective rooting depth = 8m; $r_a$=0.1,$r_b$=0.1) as compared to 'shallow rooting' (e.g effective rooting depth = 2; $r_a$=1,$r_b$=5) which represents a larger proportion of fine roots in upper layers (Figure 1a).

The safety-efficiency tradeoff of xylem has been widely discussed in the literature (e.g. Gleason et al. 2016; Hacke et al. 2006, 2017; Martnez-Vilalta, Sala, and Piol 2004). Given that we don't have any measurements that can be used to a generate vulnerability curve at our study site, we consult the literature (Domec et al. 2004, Barnard et al. 2011, Corcuera et al. 2011, Anderegg and Hillerislambers 2016 , Baker et al. 2019, Kilgore et al. 2021) for observed curves from sites that are as similar both in climate (e.g mean annual precipitation and temperature) and in the set of conifer species (P. Ponderosa) to our study site as possible, as well as values of xylem traits ($K_{max}$ and $P50_x$) of Ponderosa pine in temperate regions of the TRY database (Kattge et al. 2020) to determine the two hypothetical vulnerability curves representing the safe/inefficient and unsafe/efficient xylem strategies. We set the parameters of the van Genuchten model to represent these two sets of P-V and vulnerability curves as shown in Fig1b and 1c. It is worth noting that with the same $K_{max}$ and $P50$, the exact shape of the vulnerability can differ depending on the formula used and parameter values. However, this should not be an issue in our study because the vulnerability curve is mainly constrained by P50 and Kmax. Second, given that there is a large range of variation in the measured values, the effect caused by the exact shape of the curves is minor. Third, since the objective of our study is not to accurately predict mortality, but rather to examine the effect of different combinations of stoma, xylem, and

root strategies, even if the shape of our vulnerability curve is not the most accurate, as long as the curve captures the overall pattern of the pressure-conductivity relation, it will not affect the relative outcome of this study.

We follow the theory of Skelton et al. (2015) to define safe vs. efficient stomatal strategy. In FATES-Hydro, there are two key stomatal parameters: $P50_{gs}$ and $a_{gs}$. Here, we only vary $P50_{gs}$ while keeping $a_{gs}$ as a constant because the objective here is to choose the parameters that are relatively well understood and to catch the safe vs. risky strategies as described by Skelton et al. (2015) rather than exhaust the parameter space within the model. In essence, the different combinations of $P50_{gs}$ and the shape parameter ($a_{gs}$) can generate similar stomatal response curves. For example, a small negative $P50_{gs}$ with a small $a_{gs}$ would result in a flat stomatal response curve, which is similar to a large negative $P50_{gs}$ combined with a large $a_{gs}$. Further, $P50_{gs}$ is well understood and has more observed data, while $a_{gs}$ is less studied and barely has any observed data. With a given $a_{gs}$, the variance of $P50_{gs}$ for a given $P_{xylem}$ value, controls the degree of embolism risk, from a 'risky' strategy, where $P50_{gs}$ is equal to or lower than $P_{xylem}$, to a 'conservative' strategy, where $P50_{gs}$ is higher than $P_{xylem}$. The $P_{xylem}$s in Skelton et al.'s (2015) are for Fynbos species, therefore are not appropriate for our study because our species are pine trees, a woody plant. Trees have woody tissue, which contributes to strengthening the conduits and makes them less likely to collapse when embolized, hence allow their stomata to be riskier than those of herbaceous plants. From the observed $P50_{gs}$ and xylem traits of closely related pine species in the TRY database (Kattge et al. 2020) and elsewhere in the literature (Bartlett et al. 2016), as well as the observed soil water potential at the study site, we choose to vary $P50_{gs}$ between $P50_{xylem}$ and $P20_{xylem}$, (correspondingly the point at which xylem have lost 50% and 20% of their maximum conductivity).

The emergent behavior of FATES or any model with dynamic ecosystem structure can make analysis of physiological rate variation difficult, as the stand structure will respond and thus also vary when parameters are changed. Here, we want to first understand the direct trait control in the absence of structural differences. To overcome complications of the dynamic structure, we use a reduced complexity configuration for running the model which we refer to as 'static stand structure' mode. To investigate dynamic competitive effects when growth and mortality will be the next step. In this mode, the stand structure is initialized from observed

forest census data, and subsequently is fixed, i.e. the model does not permit plant growth or death to change the vegetation structure. This allows the direct assessment of hydraulic and physiological parameter variation in the model without the consequent feedback loops associated with varying ecosystem structure. The stand structure is initialized with census data from the CZ2 site (Table S1) and thus includes multiple cohorts of different sized trees. Because this type of model configuration ignores prognostic plant mortality, in the interest of being able to compare across simulations where mortality rates might otherwise be very high, we use the loss of xylem conductivity as a measure of mortality risk of conifer trees at CZ2, which has widely been used as an indicator of drought mortality of forest (e.g. Hammond et al., 2019).

To force the model with an atmospheric upper boundary, we use the Multivariate Adaptive Constructed Analogs (MACA) climate data (Abatzoglou and Brown 2012) from 2008 – 2015 of a 4km x 4km grid covers the study area. The daily average MACA data are disaggregated to 3-hourly climate data (see Appendix S2 in Buotte et al. 2018 for detail). We set the initial soil water content to be 75% of saturated water content, close to field capacity. We believe this is a realistic value because the model is initialized in January, when the study area has high precipitation and trees are all in a dormant status, and in a year when there is not drought. We also tried to initialize the soil with higher water content (e.g. saturation), but did not find any differences, as the extra water drained quickly in the winter when transpiration is low.

## 3. Results

### 3.1 Sensitivity of GPP and ET to parameter perturbations

The parameter sensitivity analysis revealed that in a monthly mean flux comparison, the simulations with deep roots provided a better match to the overall observed pattern of the GPP and ET (Figure 2). In general, the simulated transpiration contributed 90% of the ET. The deep-rooted cases more accurately captured the seasonality (e.g., the peak time) and the declining trend of observed GPP from 2011 to 2015. The deep-rooted cases also matched the observed ET fairly well. The simulated GPP of shallow-rooted cases was higher than the observed values during wet seasons (Dec. to Mar.) but much lower than those during the dry season of the predrought period. Overall, the simulated ET of shallow-rooted cases was lower than the observed values. To quantify this assessment, we computed the RMSE from the hourly mean

418 GPP and ET of each month and each year of all 40 cases (Figure S2). We chose the RMSE as it
419 is a common and compact metric for assessing model performance, though we note that other
420 metrics could in principle be used, each of which has different advantages and disadvantages
421 (e.g., Collier et al., 2018). The RMSE of the GPP and ET decreased with both effective rooting
422 depth and P50gs for both xylem strategies (Figure 3). The P50gs had less of an impact on the
423 RMSE of the GPP for the case with safe xylem than on that of the GPP for the case with efficient
424 xylem. In terms of the GPP, the effective rooting depth of 6.5 m provided the best fit, as
425 indicated by the darkest color (GPP RMSE = 1.12 $gC/m^2/s$, ET RMSE = 250 $W/m^2$). This
426 underscores the importance of deep roots in maintaining transpiration and photosynthesis during
427 the dry season as well as the role of deep roots in increasing the relative decline in these fluxes
428 during droughts.

429 Among the parameters that we varied in the sensitivity analysis, the vertical root
430 distribution had the largest impact on the GPP and ET at CZ2. Figure 2a–b show the monthly
431 mean GPP and ET of the end members of the sensitivity analysis (see Figure S1 for the complete
432 set of outcomes). We acknowledge that the variation in rooting depth across the ensemble was
433 large; however, we also highlight that so too was the uncertainty in plant rooting depth, and also
434 that the uncertainty in rooting depth was less well-quantified than other plant traits (e.g., P50),
435 such that this wide variation reflects a real and deep uncertainty in plant rooting profiles. Deep
436 roots resulted in a substantially higher GPP and transpiration during normal years (2011 and
437 2012). During long-term droughts, when deep soil moisture was depleted, the relative advantage
438 of deep roots over shallow roots was reduced. Shallow roots resulted in a substantially lower
439 GPP and transpiration during the dry season (Aug. to Oct.), with the seasonal maximum
440 occurring earlier – in May – as opposed to July with deep-rooted cases. The shallow-rooted cases
441 also had a much lower GPP and ET during the dry seasons of the predrought period. During the
442 late stages of drought (2014 and 2015), the GPP and ET of the different cases became more
443 similar between the shallow- and deep-rooted cases.

444 The second most important set of parameters for controlling carbon and water fluxes are
445 those that govern the stomatal strategy. The simulations with a riskier strategy ($P50_{gs} = P50_x$)
446 provided a higher GPP and ET than those with a safer strategy ($P50_{gs} = P20_x$) during predrought
447 periods and the early stage of the drought (2011 to 2013), but they provided a slightly lower GPP

448 and ET in the late stage (2014 and 2015) for the deep-rooted cases. However, risky stomata
449 provided a slightly higher GPP and ET at all times for shallow-rooted cases. The xylem strategy
450 had the smallest effect on the GPP and ET of the parameters that we varied (e.g., the RMSEs of
451 ET were both approximately 260 W/m$^2$ for safe and efficient xylem, respectively, with P50gs =
452 P20x and an effective rooting depth of 8 m). In deep-rooted cases, the safe xylem and efficient
453 xylem strategies resulted in an almost identical GPP and ET, which can be seen in the widest
454 overlap between the dashed and solid lines in Figure 1. In shallow-rooted cases with safe
455 stomata, safe xylem generated a slightly higher GPP and ET than efficient xylem. In addition, the
456 strength of the effects of stomatal and xylem strategies also depend on the rooting depth. The
457 deeper the effective rooting depth, the less significant the impacts of stomatal strategy (Figure
458 S1).

459

460 3.2 Sensitivity of plant water status to parameter perturbations

461 We examined the impact of vertical root distributions and stomatal and xylem strategies on
462 the seasonal variation of the following three plant physiological variables, which served as
463 indices of plant water stress (Figure 4): the fraction loss of xylem conductivity of the stem (SFL),
464 leaf water potential (LWP), and an overall absorbing root water potential (AWP). In the model,
465 absorbing roots in different soil layers had different water potentials associated with the soil
466 water potential of that layer. We calculated a cohort-level effective AWP as the root-fraction-
467 weighted average of water potential in absorbing roots across all soil layers. Thus, the AWP
468 represents the overall rhizosphere soil moisture condition that is sensed by the tree. These
469 physiological variables were tracked for each cohort. In any given case, the differences in these
470 variables among differently sized cohorts were negligible (Figure S3). Therefore, we present the
471 outcome of all cohorts with a diameter at breast height (DBH) between 50 and 60 cm, the size
472 class that was most abundant at CZ2.

473 Stomatal and rooting strategies together controlled the loss of xylem conductivity during
474 the dry season of the predrought period and the whole period of the long-term drought (Figure
475 4a). In all cases, the xylem conductivity reached a maximum during the wet season (Dec. to
476 Jan.), started to decline during the growing season (Apr. to Jun.), and then reached its minimum
477 in the dry season. With the same stomatal strategy, deep roots led to a less extreme loss of xylem

conductivity than shallow roots. A deep rooting strategy was also able to maintain xylem conductivity with very little seasonal loss during the predrought period; however, as deep soil moisture was depleted, this effect was reduced. With a shallow rooting profile, the xylem conductivity started to decline earlier, and the minimum was much lower than that of a deep rooting profile. For example, with risky stomata, the minimum fraction of xylem conductivity in deep-rooted cases in 2012 was 0.4, but it was lower than 0.2 with shallow roots. Unlike deep-rooted cases, the seasonal variation of the loss of xylem conductivity did not differ too much during predrought and drought periods in shallow-rooted cases. Furthermore, during the very late stage of the drought, deep-rooted cases had a lower fraction of xylem conductivity than shallow-rooted cases (e.g., in Jan. 2015).

In general, risky stomata allowed a greater loss of xylem conductivity (K/Kmax) than safe stomata, but the extent depended on the vertical root distribution. The effect of stomatal strategy was more obvious in shallow-rooted cases. Risky stomata combined with shallow roots resulted in an increase in the duration of the 50% loss of xylem conductivity as well as the maximum loss of xylem conductivity during the dry season. With a deep rooting strategy, the difference in the percentage loss of xylem conductivity between safe and risky stomatal cases increased with the progression of the drought; however, with a shallow rooting strategy, this difference remained approximately the same over time. In addition, in 2011, a very wet year with deep roots, a safe xylem strategy was able to maintain the maximum xylem conductivity even during the dry season (Figure 4a). The impact of the xylem strategy on the percentage loss of xylem conductivity was relatively weak. In both deep- and shallow-rooted cases, trees with safe xylem lost less xylem conductivity during the wet season but more conductivity during the dry season.

The safe stomata and safe xylem cases for both deep- and shallow-rooted trees experienced greater declines in stem conductivity compared with the safe stomata and efficient xylem for the corresponding rooting depths (Figure 4a). This is because with safe stomata, trees operate at the right end of the vulnerability curve displayed in Figure 1b, where the hydraulic conductivity of efficient xylem is much higher than that of safe xylem. Thus, when the same amount of water is transpired, efficient xylem will lose less water potential than safe xylem. This keeps the xylem water potential of a plant with efficient xylem higher than that of one with safe xylem, and consequently, it also keeps the xylem conductivity, $K$, higher. This is also because we set $P50_{gs}$

508 based on $P_{xylem}$; thus, the $P50_{gs}$ of safe stomata for plants with efficient xylem was higher (less
509 negative) than that of plants with safe xylem, resulting in lower transpiration rates, which in turn
510 reduced the loss of xylem water potential. As a result, plants with both safe stomata and efficient
511 xylem not only transpired less water but also lost less water potential per volume of transpired
512 water. Together, these two mechanisms contributed to keeping the xylem conductivity of the
513 efficient xylem cases higher.

514 In addition, stomatal, rooting, and xylem strategies had similar impacts on the seasonal
515 variation of both leaf and fine root water potentials (Figure 4c and 4d). Leaf and fine root water
516 potentials peaked during the winter, then started to decline in early spring, and reached their
517 lowest point in the dry season. Deep roots, safe stomata, and safe xylem traits all contributed to
518 the maintenance of higher leaf and fine root water potentials during the growing and dry seasons.
519 With deep roots, there was less of a difference in leaf and fine root water potentials between
520 stomatal and xylem strategies in the very wet year of 2011. Plants that combine safe stomata
521 and/or safe xylem with deep roots were able to keep the leaf and fine root water potentials
522 relatively high (less than -5 Mpa) during the dry season of the drought period. However, while
523 plants that combine risky stomata or efficient xylem with deep roots could keep the dry season
524 leaf water potential above -5 Mpa during the predrought period, their traits led to the dry season
525 leaf water potential dropping below -8 Mpa or even -10 Mpa during the drought period. In both
526 deep- and shallow-rooted cases, safe xylem led to much lower leaf and fine root water potentials
527 during the dry season. The seasonal and inter-annual variation of fine root water potentials was
528 almost identical to the leaf water potential, except that the water potential of fine roots was
529 slightly higher (~ 0.5 Mpa) than the leaf water potential.

530 3.3 Sensitivity of subsurface hydrology to parameter perturbations

531 In the simulation outcomes, the vertical root distributions again had the largest impact on
532 hydrological processes, subsurface water content, and how they changed over the drought. With
533 deep roots, there was less drainage loss from surface and subsurface runoff compared with
534 shallow roots, especially during the growing season (Figure 5a, c, e, and g). The subsurface
535 water content exhibited different vertical and temporal patterns between the cases with different
536 vertical root distributions. In the deep-rooted cases, during the predrought period, the water
537 content in the deepest layers fluctuated between wet and dry seasons; during the first year of the

drought, the water content of the deepest layers (6–8 m) slightly increased during the wet season, but as the drought progressed, the soil water content became consistently depleted in the middle and deep layers (5–8 m) and only the shallow layer's (<0.16 m) water content increased during the wet season. In the shallow-rooted cases (Figure 5b, d, f, and h), soil moisture in the surface layers (top 2 m) exhibited seasonal variation, but this became weaker with depth. Moreover, the soil moisture at 6–8 m depth stayed consistently high throughout the year during the predrought period and remained slightly low throughout the entire drought period, while the water content of the middle and upper layers of the shallow-rooted case exhibited a similar pattern of seasonal variation before and during the drought.

The stomatal strategy, as quantified by $P50_{gs}$, had a weak impact on hydrological processes and soil moisture. In both deep- and shallow-rooted cases, riskier stomata led to a slightly lower total subsurface water content (Figure 6a). The effect of $P50_{gs}$ was less significant during the predrought period for both the deep- and shallow-rooted cases and became more significant as the drought progressed. The effect of $P50_{gs}$ on total subsurface water content was less significant in shallow-rooted cases. Figure 5c presents the effect of $P50_{gs}$ on the water content of shallow and deep soil layers. In both the shallow- and deep-rooted cases, increasing $P50_{gs}$ had a negligible impact on the water content of the shallow layers during both the predrought and drought periods (Figure 5c, left). For deeper layers, in the shallow-rooted case, $P50_{gs}$ had no impact on the water content at any time; in the deep-rooted cases, a risky $P50_{gs}$ resulted in a lower dry season water content of deep layers (7–8 m) during the predrought period (as indicated by the red cycles in Figure 5a and 5c), but it decreased the water content of those layers year-round during the drought period (Figure 5a and 5e). In deep-rooted cases, safe stomata with efficient xylem led to a slightly higher water content in deep layers (5–8 m) during the predrought period and in shallow layers (0–3 m) during the drought period (Figure 6a). Risky stomata with safe xylem in deep-rooted cases were most effective at accessing soil water. Although the soil water contents were generally high in shallow-rooted cases, stomatal and xylem strategies exhibited a similar impact on soil water storage as those in deep-rooted cases (Figure S4).

Furthermore, simulations with deep roots resulted in almost no loss of soil water to drainage during the dry season in normal years or during the whole drought period; by contrast,

in simulations with shallow roots, the drainage loss was high during the predrought period and decreased through the drought period, but still with some runoff even at the end of the period (Figure 6a). The observed total annual runoff from the 2008–2011 predrought period was approximately 250 mm/year, but it was zero during the 2012–2015 drought period (from Figure 4; Bales et al. 2018). This observed difference in runoff between the predrought (~290 mm/year, 2011–2012) and drought periods (~0 mm/year) in the deep-rooted case was consistent with the predicted pattern. During the predrought period, the wet season total subsurface water contents from December to February were similar between the cases with deep and shallow roots; however, during the dry season (from June to Sep.) the total subsurface water content with shallow roots was substantially higher than the case with deep roots (Figure 6b).

## 4. Discussion

### 4.1 Vertical root distribution as the first-order control

The outcomes of our simulations indicated that the vertical root distribution exerted first-order control over both ecosystem-level fluxes and plant physiology at CZ2. This dominance of the rooting strategy over other hydraulic traits is related to the nature of the rainfall pattern in the Mediterranean-type climate of that region. The CZ2 site receives effectively all of its rain during the winter. This water is stored in the soil column and slowly released through the growing season. The root zone soil moisture exhibits strong seasonal variation, which constrains plant water use and gas exchange as a function of the gradual drying of the soil column (Bales et al., 2018). In the model, the stomatal behavior was controlled by the leaf water potential, which itself was strongly affected by the root zone soil moisture. In our simulations, the daytime average leaf water potential of a 55cm DBH cohort was well correlated with the fine root water potential and was always approximately 0.5 Mpa lower (Figure S5). This offset is consistent with the relationship between the mid-day leaf water potential and predawn leaf water potential found by Martínez-Vilalta et al. (2014) at the global scale.

With deep roots, trees used more subsurface storage capacity at the CZ2 site. In wet years such as 2011, the root zone water potential of deep-rooted trees was maintained relatively high (Figure 4b) and the trees operated at the upper end of their vulnerability curve throughout the year, with a typical loss of conductivity of 10% (Figure 7). Therefore, we did not observe much

of an effect of stomatal strategy on the GPP and transpiration in wet years. At the upper end of the vulnerability curve, stomata were fully open regardless of stomatal strategy (either safe or risky). When the drought began in late 2012, annual rainfall fell below the total root zone storage, and therefore, the deep storage remained depleted throughout the year. During the drought, the deep-rooted trees were able to operate at the high end of the vulnerability curve in the wet season, when the rainfall recharged the surface layer. As the surface layers dried, water potential then gradually fell to the lower end of the vulnerability curve; consequently, photosynthesis and transpiration started to drop as the dry season progressed. With risky stomata, trees can drive soil moisture to lower values. This is why we observed the difference in the effect on the GPP and transpiration between different stomatal strategies during the dry season as the drought progressed.

With shallow roots, trees can only use surface soil moisture storage. As a result, the surface water storage was quickly used up after the wet season, and the root zone water potential dropped near the low end of the vulnerability curve during the dry season. Thus, shallow-rooted trees operated along the full extent of the vulnerability curve year-round, during both predrought and drought periods. Therefore, for the deep-rooted cases, we did not observe a strong effect of stomatal strategy on the GPP and transpiration during the wet season; however, unlike the deep-rooted cases, the effect of stomatal strategy on the GPP and transpiration during the dry season could be observed throughout the whole simulation period.

Rooting strategies greatly control the spatial pattern of vertical soil water content (Figure 5). With deep roots, the vertical soil moisture variation was more homogeneous due to the extensive root distribution. With shallow roots, the soil became extremely dry at the surface (<1 m) and extremely wet in deep layers (>5 m) as a result of the aggregated root distribution in the upper layers. This finding is similar to that of Agee et al. (2021), who found that extensive lateral root spreading results in homogeneous soil moisture distribution. The homogeneous soil moisture pattern may contribute to a more energy-efficient system that reduces plant water stress (Agee et al. 2021) because it minimizes the loss of energy dissipation through water transport (Hildebrandt et al. 2016). Both our study and that of Agee et al. (2021) emphasize the importance of the means by which the root distributions determine how the subsurface storage is used.

627 Given the shape of the vulnerability curves, plants stopped transpiring in all simulations
628 when their leaf water potential reached approximately −10 MPa with efficient xylem or −15 MPa
629 with safe xylem, depending on their stomatal strategy (Figure 7). Because we held the stand
630 structure and leaf area constant to allow comparisons between cases, the simulated leaf water
631 potential of the shallow-rooted, risky stomata combination could reach as low as −15 Mpa
632 (Figure 4b) during dry seasons, even during the predrought period, which is well below the
633 lowest possible leaf water potential observed (−10 Mpa; Vesala et al., 2017). Leaves would
634 likely be wilted before the water potential drops below −10 MPa, and the tree would already
635 have shed the leaves due to canopy desiccation. However, we specifically did not permit that in
636 these simulations to keep the different cases comparable. Although it might be unrealistic, the
637 leaf water potential can serve as an indicator of the degree of canopy desiccation. With no or
638 very few leaves, trees would rely on stored carbon to support respiratory demand until the wet
639 season arrives to regrow leaves. Depending on the duration of the dry season, trees may exhaust
640 their stored carbon and die from carbon starvation. While risky stomata can generate a higher
641 GPP (Figure 1a), they also result in a longer duration of more negative leaf water potential
642 (Figure 4b). This suggests that shallow-rooted pines at CZ2 with risky stomata would benefit
643 from allocating more net primary productivity to their storage pools rather than growth in order
644 to reduce carbon-starvation mortality. Therefore, even though the model generated unrealistically
645 low leaf water potentials, the extent and duration of these simulated potentials allowed us to gain
646 some insights into the interaction of plants' hydraulic strategies and the life history strategies of
647 conifer trees under a Mediterranean-type climate. Furthermore, the unrealistic leaf water
648 potential from the shallow root simulations indicated that the trees at that site must have very
649 deep roots to exist there, which is in agreement with the conclusions of Goulden and Bales
650 (2019).

651 In this simulation, the impacts of xylem traits on the GPP and ET were weak and subtle.
652 This was the result of the relative position of the two vulnerability curves, particularly the
653 intersection of the two vulnerability curves in absolute conductivity. When the absolute
654 conductivity was plotted as a function of pressure (Figure 1b and solid lines in Figure S6), we
655 observed, on the left side of the intersection, that the safe xylem was not only safe but also
656 efficient; thus, a safety–efficiency tradeoff of xylem only occurred on the right side of the
657 intersection point. Therefore, in shallow-rooted cases, when the root zone water content—and

hence the plant water status—is low, safe xylem can generate a slightly higher GPP and ET than unsafe xylem. Furthermore, the two pressure–conductivity curves diverged mainly at the wet end (corresponding to the wet season). This is likely to be because the xylem structures of conifers are very similar and the range of variation of xylem traits in the sensitivity analysis was limited to the dominant species at the site. Therefore, the difference in the xylem traits of conifers does not cause significant impacts on the ecosystem-level fluxes under the Mediterranean-type climate of CZ2, which are constrained by energy during the wet season (Goulden et al., 2012). In addition, the maximum rates of GPP and ET are co-constrained by the stand density, total leaf area, maximum stomatal conductance, and VPD. In this study, we used the static stand structure mode of FATES-Hydro, whereby the stand density and the total leaf biomass (so as total leaf area) of the trees were held constant. This further limited the effect of xylem traits on the GPP and ET.

## 4.2 Balancing productivity and mortality risk

The hydraulic traits that contribute to high carbon fixation rates often make trees more susceptible to drought. Stomatal strategy ($P50_{gs}$) can have both positive and negative impacts on trees, creating a tradeoff in the balance between productivity and physiological stress. The risky stomata ($P50_{gs} = P50_{x}$) can generate a higher GPP but also result in a greater loss of xylem conductivity and lower leaf water potential. The tradeoff varies depending on the plant's root strategy (i.e., having a deep vs. a shallow root distribution) and moisture state.

To better understand the tradeoff between productivity and mortality risk, we plotted the simulated annual average GPP for each year against the fraction of conductivity (K/Kmax) of a 55 cm DBH cohort for two scenarios – deep roots (Figure 8a) and shallow roots (Figure 8b) – with different combinations of xylem and stomatal strategies. In both scenarios, for each pair of xylem and stomatal strategies, the GPP per tree increased almost linearly with K/Kmax. However, as the safety of the stomata increased, the GPP declined faster with the loss of conductivity. This response was stronger in deep-rooted scenarios. Having efficient xylem only slightly increased the steepness of the lines. The stomatal strategies thus represented points along a gradient of the tradeoff between growth and mortality risk; the safer the stomata, the more the GPP was traded to reduce mortality risk.

688 Along this tradeoff space, the point at which trees can maximize their net carbon gains
689 likely depends on the xylem traits. Studies have demonstrated that trees may temporarily lose
690 xylem conductivity during mild droughts, which can recover once soil water becomes available.
691 However, under extreme drought, their xylem could collapse and permanently damage the xylem
692 conduits. In this case, trees rely on new sapwood growth to support transpiration (Brodribb et al.
693 2010, Anderegg et al. 2013). At one extreme, if the stomatal behavior is too safe, it will produce
694 a low GPP and the tree will be outcompeted for light due to faster-growing neighbors; however,
695 at the other extreme, if the stomata behave very aggressively (risky), this will produce a high
696 GPP but also empty the subsurface storage quickly, consequently leading to a prolonged dry
697 period of soil moisture. This would lead to substantial xylem damage (and/or root death), and
698 then the carbon required to grow new sapwood (or roots) could exceed the benefits from the
699 additional GPP. Thus, the optimal location along the gradient would probably be located slightly
700 below the K/Kmax associated with that critical xylem water potential. Currently, the xylem
701 refilling and associated carbon cost are not incorporated into FATES-Hydro. These two
702 processes should be implemented in the model to obtain an enhanced understanding of the
703 water–carbon balance, which remains for future work.

704 In the deep-rooted scenario, the values of the predrought period and early drought stage
705 were clustered in the upper-right corner, above a K/Kmax of 0.6 (Figure 8a). In this region, the
706 stress from the loss of xylem conductivity likely would not be high enough to cause severe
707 consequences if we were to use a 50% loss of xylem conductivity as the threshold for mortality
708 and/or permanent xylem damage. The deep-rooted tree can thus benefit by trading less GPP for
709 maintaining xylem conductivity with a risky/more productive stomatal strategy during normal
710 years. However, during the late stages of the drought (2014 and 2015), the conductivity values
711 became much lower. If this megadrought stopped earlier (e.g., if it were a mild drought that only
712 lasted for two years), then the additional GPP obtained from risky stomata may outweigh the
713 carbon cost of repairing xylem damage. This suggests that if the 2012–2015 drought was not
714 common in California, then natural selection might favor the risky/more productive stomatal
715 strategy for deep-rooted trees. However, the same strategy would also expose trees to a high
716 mortality risk during severe droughts.

In the shallow-rooted case (Figure 8b), the values were all clustered lower and to the left compared with the deep-rooted scenario, irrespective of the drought status. Thus, for shallow roots, risky/more productive stomatal behavior resulted in a similarly high mortality risk during both the predrought and drought periods. Accordingly, under the long-term climate conditions found at CZ2, regardless of whether severe droughts were frequent or not, the only shallow-rooted trees that could persist would have to follow the safe and less-productive stomatal strategy. Therefore, safe and less-productive stomata also protect shallow-rooted trees from mortality risk during drought.

The model outcome indicated that under drier root zone soil conditions, if pines were to follow a shallow rooting strategy, they would benefit from a safer stomatal strategy with more conservative water use; by contrast, if they were to follow a deep rooting strategy, they would benefit from riskier stomata. This is consistent with Anderegg et al.'s (2016) finding regarding the relative stomatal conductance (gs) across elevation. They found that at a low elevation (lower precipitation) site, Ponderosa pine had lower relative stomatal conductance and less loss of xylem conductivity, equivalent to safer stomata in our study, while at a mid-elevation (higher precipitation) site, it had higher relative stomatal conductance and a greater loss of xylem conductivity, equivalent to risky stomata in our study. The simulation results are consistent with the idea that the CZ2 region is dominated by deep-rooted trees, which is supported by previous studies. In situ measurements of regolith structure (particularly the porosity) indicate that at CZ2, there is a layer of thick, semi-weathered bedrock that allows the trees to grow deep roots (Holbrook et al., 2014). Growing deep roots to access rock moisture to support plant water use was also observed in the Eel River CZO catchment (Rempe et al., 2018), another Mediterranean-type ecosystem along the west coast. Observed net $CO_2$ exchange and ET during the predrought period suggested that during a wet year, deep moisture supported summer transpiration and productivity when the upper layer moisture was low (Goulden et al. 2015). Because the deep rooting strategy is sufficient in most cases for avoiding the main effects of dry seasons and short droughts, and because, conditional on having deep roots, the risky stomatal strategy confers a productivity advantage at a little increased risk of vulnerability, we would expect plants with these traits to dominate. However, under extreme cases such as the 2012–2015 drought, which ranked as one of the most severe in California in the last 1200 years (Lu et al. 2019), we would expect plants with this deep-rooted, risky stomatal strategy to be highly vulnerable to drought,

748 which is consistent with the approximately 90% mortality of the pine observed at CZ2 during the
749 drought (Fettig et al. 2019). The water balance of the catchment based on long-term observation
750 from precipitation, stream flow, and ET (Bales et al. 2018, Goulden and Bales 2019) also
751 supports that it was the slow depletion of deep moisture that caused tree mortality in the late
752 stage of the prolonged 2012–2015 drought.

753 The findings of our study indicate that future drought mortality will likely occur in
754 ecosystems that are limited by water and other factors. In such ecosystems, trees can benefit
755 from having more efficient but less safe hydraulic traits, as they allow them to be more
756 competitive for water and bring in a higher GPP. The extra carbon gain can be used to develop
757 measures for dealing with other constraining factors, such as increasing stored carbon to lower
758 the risk of carbon starvation, building thicker bark to resist fire, and growing more roots, which
759 further enhance their capacity to compete for water.

760 **5. Conclusions**

761 Our analysis indicates that root distribution can affect the most competitive stomatal traits.
762 In a Mediterranean-type climate where the supply of energy and water is desynchronized and
763 accessible subsurface water storage capacity is close to annual precipitation, deep roots
764 combined with risky stomata represent a beneficial strategy for high productivity in normal years
765 with low mortality risk; however, this strategy exposes trees to a high mortality risk during
766 multi-year droughts. While such a strategy enables trees to fully use subsurface storage and
767 precipitation for productivity over regular years, the lack of deep water storage recharge during
768 droughts exposes trees to high drought stress and makes this strategy unfavorable under severe
769 and prolonged drought. By contrast, shallow roots combined with safe stomata represent a
770 strategy for drought resistance, albeit at the cost of considerably reduced productivity, as such a
771 combination only allows trees to use shallow subsurface storage while leaving deep moisture
772 untouched; thus, less precipitation is used for productivity. However, this strategy leaves trees
773 less susceptible to drought-induced mortality should the deep reservoir be depleted. By contrast,
774 shallow roots with risky stomata lead to high mortality even during nondrought years, making
775 this an uncompetitive combination at the site. These results suggest that stomatal strategy is
776 controlled by root zone soil moisture and regulated by root distribution in that region. Thus, our

777 study underscores the importance of considering plant rooting and hydraulic strategies within the
778 larger context of plant ecological strategies.

779

780 **Author contribution**

781 JD and CDK design the study and write the MS. JD conducted the simulation. PB, RB, MG
782 provided model input data. BC, CDK, RF, RK, CX, and JD wrote the code. PB, RB, BC, RF,
783 MG, RK, LK, JS, CX edited the MS.

784

785 **Acknowledgement**

786 We acknowledge support by the Director, Office of Science, Office of Biological and
787 Environmental Research of the U. S. Department of Energy under Contract DE-AC02-
788 05CH11231 through the Early Career Research Program, the University of California Laboratory
789 Fees Research Program, and National Science Foundation Southern Sierra Critical Zone
790 Observatory grant EAR-1331931. RF acknowledges funding by the European Union's Horizon
791 2020 (H2020) research and innovation program under Grant Agreement No. 101003536
792 (ESM2025 – Earth System Models for the Future) and 821003 (4C, Climate-Carbon Interactions
793 in the Coming Century)

794 **Data availability statement**

795 The FATES code (branch FATEScodeforMS1), parameter files and data that support the
796 findings of this study are openly available at ZENODO:
797 https://zenodo.org/account/settings/github/repository/JunyanDing/Rooting-and-Hydraulic-
798 strategy-of-pine-at-Sierra-CZ2- (DOI 10.5281/zenodo.5504405). The flux tower data can be
799 retrieved from the UC Merced online database (https://www.ess.uci.edu/~california/).

800 **Competing interests**

801 The authors declare no conflict of interest

## 5. References


Abatzoglou J.T. and Brown T.J. "A comparison of statistical downscaling methods suited for wildfire applications" International Journal of Climatology (2012), 32, 772-780. 2012.

Adams, H. D. et al. "Mechanisms in Drought-Induced Tree Mortality." *Nature Ecology & Evolution* 1(September). http://dx.doi.org/10.1038/s41559-017-0248-x. 2017.

Agee, E., He, L., Bisht, G., Couvreur, V., Shahbaz, P., Meunier, F. et al., 2021. Root lateral interactions drive water uptake patterns under water limitation. Adv. Water Resour., 151: 103896.

Anderegg, W.R., Plavcová, L., Anderegg, L.D., Hacke, U.G., Berry, J.A. and Field, C.B., Drought's legacy: multiyear hydraulic deterioration underlies widespread aspen forest die-off and portends increased future risk. Global change biology, 19(4), pp.1188-1196. 2013.

Anderegg, L. D. L. and Hillerislambers, J. Drought stress limits the geographic ranges of two tree species via different physiological mechanisms Glob. Chang. Biol. 22 1029–45 Online: http://dx.doi.org/10.1111/gcb.13148 . 2016

Ando, Eigo, and Kinoshita, Toshinori. "Red Light-Induced Phosphorylation of Plasma Membrane H+ -ATPase in Stomatal Guard Cells." *Plant Physiology* 178(October): 838–49. 2018.

Baker, Kathryn V., Tai, Xiaonan, Miller, Megan L, Johnson, D. M., Six co-occurring conifer species in northern Idaho exhibit a continuum of hydraulic strategies during an extreme drought year, AoB PLANTS, Volume 11, Issue 5, October 2019, plz056,

Bales, Roger et al. "Spatially Distributed Water-Balance and Meteorological Data from the Rain – Snow Transition , Southern Sierra Nevada , California." : 1795–1805. 2018.

Bales, Roger et al. 2018. "Mechanisms Controlling the Impact of Multi-Year Drought on Mountain Hydrology." *Scientific Reports* (December 2017): 1–8.

Ball, J. Timothy, Ian E. Woodrow, and Joseph A. Berry. "A model predicting stomatal conductance and its contribution to the control of photosynthesis under different environmental conditions." Progress in photosynthesis research. Springer, Dordrecht, 221-224. 1987.

Barnard, DM, Meinzer, FC, Lachenbruch, B., McCulloh, KA, Johnson, DM, Woodruff, D.R. Climate-related trends in sapwood biophysical properties in two conifers: avoidance of hydraulic dysfunction through coordinated adjustments in xylem efficiency, safety and capacitance. Plant Cell Environ. Apr;34(4):643-54. doi: 10.1111/j.1365-3040.2010.02269.x. Epub 2011 Feb 11. PMID: 21309793. 2011

Bartlett, M.K., Klein, T., Jansen, S., Choat, B. and Sack, L., The correlations and sequence of plant stomatal, hydraulic, and wilting responses to drought. Proceedings of the National Academy of Sciences, 113(46), pp.13098-13103. 2016.

Brodribb, T.J., Bowman, D.J., Nichols, S., Delzon, S. and Burlett, R., 2010. Xylem function and growth rate interact to determine recovery rates after exposure to extreme water deficit. New Phytologist, 188(2), pp.533-542.

Buotte, Polly C., Samuel Levis, Beverly E. Law, Tara W. Hudiburg, David E. Rupp, and Jeffery J. Kent. "Near - Future Forest Vulnerability to Drought and Fire Varies across the Western United States." (July):1–14. 2018.

Canadell, J.G., Le Quéré, C., Raupach, M.R., Field, C.B., Buitenhuis, E.T., Ciais, P., Conway, T.J., Gillett, N.P., Houghton, R.A. and Marland, G., Contributions to accelerating atmospheric CO2 growth from economic activity, carbon intensity, and efficiency of natural sinks. *Proceedings of the national academy of sciences*, *104*(47), pp.18866-18870. 2007.

Choat, Brendan, and Jarmila Pittermann. "New Insights into Bordered Pit Structure and Cavitation Resistance in Angiosperms and Conifers." *New Phytologist*: 555–57. 2009.

Christoffersen, B. O. et al. "Linking Hydraulic Traits to Tropical Forest Function in a Size-Structured and Trait-Driven Model (TFS v . 1-Hydro )." : 4227–55. 2016.

Coley, P.D., Bryant, J.P. and Chapin, F.S., Resource availability and plant antiherbivore defense. *Science*, *230*(4728), pp.895-899. 1985.

Corcuera, L., Cochard, H., Gil-Pelegrin, E. and Notivol, E., Phenotypic plasticity in mesic populations of Pinus pinaster improves resistance to xylem embolism (P 50) under severe drought. Trees, 25(6), pp.1033-1042. 2011.

Craine, J.M., Tilman, D., Wedin, D., Reich, P., Tjoelker, M. and Knops, J., Functional traits, productivity and effects on nitrogen cycling of 33 grassland species. *Functional Ecology*, *16*(5), pp.563-574. 2002.

Danabasoglu, G. et al. "The Community Earth System Model Version 2 ( CESM2 ) Journal of Advances in Modeling Earth Systems." *Journal of Advances in Modeling Earth Systems* 2: 1–35. 2020.

Domec, JC., Warren, J.M., Meinzer, F.C. *et al.* Native root xylem embolism and stomatal closure in stands of Douglas-fir and ponderosa pine: mitigation by hydraulic redistribution. *Oecologia* **141,** 7–16 https://doi.org/10.1007/s00442-004-1621-4. 2004.

Fettig, Christopher J, Leif A Mortenson, M Bu, and Patra B Fou. "Tree Mortality Following Drought in the Central and Southern Sierra Nevada, California, U.S." *Forest Ecology and Management* 432: 164–78. 2019.

Fisher, R. a. et al. "Taking off the Training Wheels: The Properties of a Dynamic Vegetation Model without Climate Envelopes, CLM4.5(ED)." *Geoscientific Model Development* 8(11): 3593–3619. 2015.

Gaylord, M.L., Kolb, T.E. and McDowell, N.G.,. Mechanisms of piñon pine mortality after severe drought: a retrospective study of mature trees. *Tree physiology*, *35*(8), pp.806-816. 2015

Geen, Anthony Toby O et al. "Southern Sierra Critical Zone Observatory and Kings River Experimental Watersheds : A Synthesis of Measurements , New Insights , and Future Directions." *Vadose Zone J. Advancing Critical Zone ScienceAdvancing Critical Zone Science*. 2018.

Gleason, Sean M., Mark Westoby, Steven Jansen, Brendan Choat, Uwe G. Hacke, Robert B.

Pratt, Radika Bhaskar, Tim J. Brodribb, Sandra J. Bucci, Kun Fang Cao, Hervé Cochard, Sylvain Delzon, Jean Christophe Domec, Ze Xin Fan, Taylor S. Feild, Anna L. Jacobsen, Daniel M. Johnson, Frederic Lens, Hafiz Maherali, Jordi Martínez-Vilalta, Stefan Mayr, Katherine A. Mcculloh, Maurizio Mencuccini, Patrick J. Mitchell, Hugh Morris, Andrea Nardini, Jarmila Pittermann, Lenka Plavcová, Stefan G. Schreiber, John S. Sperry, Ian J. Wright, and Amy E. Zanne. "Weak Tradeoff between Xylem Safety and Xylem-Specific Hydraulic Efficiency across the World's Woody Plant Species." *New Phytologist* 209(1):123–36. 2016.

Golaz, Jean-Christophe, Luke P. Van Roekel, Xue Zheng, Andrew F. Roberts, Jonathan D. Wolfe, Wuyin Lin, Andrew M. Bradley et al. "The DOE E3SM Model Version 2: overview of the physical model and initial model evaluation." Journal of Advances in Modeling Earth Systems 14, no. 12 (2022).

Goulden, M L et al. "Evapotranspiration along an Elevation Gradient in California ' s Sierra Nevada." *Journal of Geophysical Research* 117(1): 1–13. 2015.

Goulden, M L, and R C Bales. 2019. "California Forest Die-off Linked to Multi-Year Deep Soil Drying in 2012–2015 Drought." *Nature Geoscience* 12(August). http://dx.doi.org/10.1038/s41561-019-0388-5.

Grime, J.P., Evidence for the existence of three primary strategies in plants and its relevance to ecological and evolutionary theory. *The American Naturalist*, *111*(982), pp.1169-1194. 1977.

Grime, J.P., Plant strategies and vegetation processes. *Plant strategies and vegetation processes.* 1979.

Hacke, Uwe G., Rachel Spicer, Stefan G. Schreiber, and Lenka Plavcová. "An Ecophysiological and Developmental Perspective on Variation in Vessel Diameter." *Plant Cell and Environment* 40(6):831–45. 2017.

Hammond, W., K. Yu$^{+}$, L. Wilson, R. Will, W.R.L. Anderegg, and H. Adams. 2019. "Dead or dying? Quantifying the point of no return from hydraulic failure in drought-induced tree mortality". *New Phytologist*. doi: 10.1111/nph.15922. Published, 05/2019

Hartmann, Henrik, Waldemar Ziegler, Olaf Kolle, and Susan Trumbore. "Thirst Beats Hunger - Declining Hydration during Drought Prevents Carbon Starvation in Norway Spruce Saplings." *New Phytologist* 200(2):340–49. 2013.

Hartung, Wolfram, Angela Sauter, and Eleonore Hose. "Abscisic Acid in the Xylem : Where Does It Come from , Where Does It Go To ?" 53(366): 27–32. 2002.

Hetherington, Alistair M, and F Ian Woodward. "The Role of Stomata in Sensing and Driving Environmental Change." *Nature* 424(August): 901–8. 2003.

Huang, J., Kautz, M., Trowbridge, A. M., Hammerbacher, A., Raffa, K. F., Adams, H. D., ... & Gershenzon, J. Tree defence and bark beetles in a drying world: carbon partitioning, functioning and modelling. *New Phytologist*, *225*(1), 26-36. (2020).

Inouea, Shin-ichiro, and Toshinori Kinoshitaa. 2017. "Blue Light Regulation of Stomatal Opening and the Plasma Membrane H+-ATPase 2." *Plant Physiology* (166): 17.

Ivanov, Valeriy Y., Lucy R. Hutyra, Steven C. Wofsy, J. William Munger, Scott R. Saleska, Raimundo C. De Oliveira, and Plínio B. De Camargo. "Root Niche Separation Can Explain Avoidance of Seasonal Drought Stress and Vulnerability of Overstory Trees to Extended Drought in a Mature Amazonian Forest." *Water Resources Research* 48(12):1–21. 2012.

Jackson, R.B., Canadell, J., Ehleringer, J.R., Mooney, H.A., Sala, O.E. and Schulze, E.D., A global analysis of root distributions for terrestrial biomes. *Oecologia*, *108*(3), pp.389-411. 1996.

Johnson, D. M., Domec, J. C., Carter Berry, Z., Schwantes, A. M., McCulloh, K. A., Woodruff, D. R., ... & McDowell, N. G. Co-occurring woody species have diverse hydraulic strategies and mortality rates during an extreme drought. *Plant, Cell & Environment*, *41*(3), 576-588. 2018.

Kattge, J., Bönisch, G., Díaz, S., Lavorel, S., Prentice, I. C., Leadley, P., Tautenhahn, S., Werner, G., et al. "TRY Plant Trait Database - Enhanced Coverage and Open Access." *Global Change Biology* 26(1):119–88. 2020.

Kelly, Anne E, and Michael L Goulden. "A Montane Mediterranean Climate Supports Year-Round Photosynthesis and High Forest Biomass." : 459–68. 2016.

Khasanova, Albina, John T. Lovell, Jason Bonnette, Xiaoyu Weng, Jerry Jenkins, Yuko Yoshinaga, Jeremy Schmutz, and Thomas E. Juenger. "The Genetic Architecture of Shoot and Root Trait Divergence between Mesic and Xeric Ecotypes of a Perennial Grass." *Frontiers in Plant Science* 10(April):1–10. 2019.

Kilgore, J.S., Jacobsen, A.L. and Telewski, F.W., Hydraulics of Pinus (subsection Ponderosae) populations across an elevation gradient in the Santa Catalina Mountains of southern Arizona. Madroño, 67(4), pp.218-226. 2021.

Klos, P Zion et al. "Subsurface Plant-Accessible Water in Mountain Ecosystems with a Mediterranean Climate." *Wiley Interdisciplinary Reviews: Water* (May 2017): 1–14. 2017.

Koch, G.W. and Fredeen, A.L., Transport challenges in tall trees. In *Vascular transport in plants* (pp. 437-456). Academic Press. 2005.

Koven, C.D., Knox, R.G., Fisher, R.A., Chambers, J.Q., Christoffersen, B.O., Davies, S.J., Detto, M., Dietze, M.C., Faybishenko, B., Holm, J. and Huang, M., Benchmarking and parameter sensitivity of physiological and vegetation dynamics using the Functionally Assembled Terrestrial Ecosystem Simulator (FATES) at Barro Colorado Island, Panama. *Biogeosciences*, *17*(11), pp.3017-3044. 2020.

Kulmatiski, Andrew and Karen H. Beard. "Root Niche Partitioning among Grasses, Saplings, and Trees Measured Using a Tracer Technique." *Oecologia* 171(1):25–37. 2013.

Lawrence, D.M., Fisher, R.A., Koven, C.D., Oleson, K.W., Swenson, S.C., Bonan, G., Collier, N., Ghimire, B., van Kampenhout, L., Kennedy, D. and Kluzek, E., The Community Land Model version 5: Description of new features, benchmarking, and impact of forcing uncertainty. *Journal of Advances in Modeling Earth Systems*, *11*(12), pp.4245-4287.

Li, S., Lens, F., Espino, S., Karimi, Z., Klepsch, M., Schenk, H.J., Schmitt, M., Schuldt, B. and

Jansen, S., 2016. Intervessel pit membrane thickness as a key determinant of embolism resistance in angiosperm xylem. *Iawa Journal*, *37*(2), pp.152-171. 2019.

Lu, Yaojie et al. 2019. "Optimal Stomatal Drought Response Shaped by Competition for Water and Hydraulic Risk Can Explain Plant Trait Covariation." (1977).

Mackay, D. S., Savoy, P. R., Grossiord, C., Tai, X., Pleban, J. R., Wang, D. R., ... & Sperry, J. S. Conifers depend on established roots during drought: results from a coupled model of carbon allocation and hydraulics. *New Phytologist*, *225*(2), 679-692. 2020.

Martínez-Vilalta, Jordi, Anna Sala, and Josep Piñol. *The Hydraulic Architecture of Pinaceae-a Review*. Vol. 171. 2004.

Matheny, Ashley M, Golnazalsadat Mirfenderesgi, and Gil Bohrer. "Trait-Based Representation of Hydrological Functional Properties of Plants in Weather and Ecosystem Models." *Plant Diversity* 39(1): 1–12. http://dx.doi.org/10.1016/j.pld.2016.10.001. 2017.

Matheny, A.M., Fiorella, R.P., Bohrer, G., Poulsen, C.J., Morin, T.H., Wunderlich, A., Vogel, C.S. and Curtis, P.S., Contrasting strategies of hydraulic control in two codominant temperate tree species. *Ecohydrology*, *10*(3), p.e1815. 2017.

Mcdowell, Nate, Nate Mcdowell, William T. Pockman, Craig D. Allen, D. David, Neil Cobb, Thomas Kolb, Jennifer Plaut, John Sperry, Adam West, David G. Williams, and Enrico A. Yepez. "Mechanisms of Plant Survival and Mortality during Drought : Why Do Some Plants Survive While Others Succumb To." 2008.

McDowell, Nate G. et al. "Evaluating Theories of Drought-Induced Vegetation Mortality Using a Multimodel – Experiment Framework." : 304–21. 2013.

Mooney, Harold and Erika Zavaleta. *Ecosystems of California*. Vol. 3. edited by H. Mooney and E. Zavaleta. Oakland, California, USA: Univ of California Press. 2003.

Mursinna, A. Rio, Erica McCormick, Kati Van Horn, Lisa Sartin, and Ashley M. Matheny. "Plant Hydraulic Trait Covariation: A Global Meta-Analysis to Reduce Degrees of Freedom in Trait-Based Hydrologic Models." *Forests* 9(8). 2018.

Oleson, Keith W et al. "Technical Description of Version 4.5 of the Community Land Model (CLM) Coordinating." In *Natl. Cent. Atmos. Res. Tech. Note*, Natl. Cent. for Atmos. Res., Boulder, Colo. 2013.

Pittermann, Jarmila, John S. Sperry, Uwe G. Hacke, James K. Wheeler, and Elzard H. Sikkema. "Inter-Tracheid Pitting and the Hydraulic Efficiency of Conifer Wood: The Role of Tracheid Allometry and Cavitation Protection." *American Journal of Botany* 93(9):1265–73. 2006.

Pittermann, Jarmila, John S. Sperry, James K. Wheeler, Uwe G. Hacke, and Elzard H. Sikkema. "Mechanical Reinforcement of Tracheids Compromises the Hydraulic Efficiency of Conifer Xylem." *Plant, Cell and Environment* 29(8):1618–28. 2006.

Pockman, W.T. and Sperry, J.S., Vulnerability to xylem cavitation and the distribution of Sonoran desert vegetation. *American journal of botany*, *87*(9), pp.1287-1299. 2000.

997 Powell, Thomas L., James K. Wheeler, Alex A. R. de Oliveira, Antonio Carlos Lola da Costa,
998 Scott R. Saleska, Patrick Meir, and Paul R. Moorcroft. “Differences in Xylem and Leaf
999 Hydraulic Traits Explain Differences in Drought Tolerance among Mature Amazon
1000 Rainforest Trees.” *Global Change Biology* 23(10):4280–93. 2017.

1001 Pratt, R.B. and Jacobsen, A.L., Conflicting demands on angiosperm xylem: tradeoffs among
1002 storage, transport and biomechanics. *Plant, Cell & Environment*, *40*(6), pp.897-913. 2017.

1003 Reich, Peter B., Ian J. Wright, Jeannine Cavender-Bares, J. M. Craine, Jacek Oleksyn, M.
1004 Westoby, and M. B. Walters. "The evolution of plant functional variation: traits, spectra,
1005 and strategies." International Journal of Plant Sciences 164, no. S3: S143-S164. (2003).

1006 Reichstein, M., Bahn, M., Mahecha, M.D., Kattge, J. and Baldocchi, D.D., Linking plant and
1007 ecosystem functional biogeography. *Proceedings of the National Academy of*
1008 *Sciences*, *111*(38), pp.13697-13702. 2014.

1009 Rodriguez-Dominguez, C.M., Buckley, T.N., Egea, G., de Cires, A., Hernandez-Santana, V.,
1010 Martorell, S. and Diaz-Espejo, A., Most stomatal closure in woody species under moderate
1011 drought can be explained by stomatal responses to leaf turgor. *Plant, Cell &*
1012 *Environment*, *39*(9), pp.2014-2026. 2016.

1013 Rowland, L., A. C. L. Da Costa, D. R. Galbraith, R. S. Oliveira, O. J. Binks, A. A. R. Oliveira,
1014 A. M. Pullen, C. E. Doughty, D. B. Metcalfe, S. S. Vasconcelos, L. V. Ferreira, Y. Malhi, J.
1015 Grace, M. Mencuccini, and P. Meir. “Death from Drought in Tropical Forests Is Triggered
1016 by Hydraulics Not Carbon Starvation.” *Nature* 528(7580):119–22. 2015.

1017 Salmon, Yann, José M. Torres-Ruiz, Rafael Poyatos, Jordi Martinez-Vilalta, Patrick Meir, Hervé
1018 Cochard, and Maurizio Mencuccini. “Balancing the Risks of Hydraulic Failure and Carbon
1019 Starvation: A Twig Scale Analysis in Declining Scots Pine.” *Plant Cell and Environment*
1020 38(12):2575–88. 2015.

1021 Sauter, Angela, W J Davies, Wolfram Hartung, and Lehrstuhl Botanik I. “The Long-Distance
1022 Abscisic Acid Signal in the Droughted Plant : The Fate of the Hormone on Its Way from
1023 Root to Shoot.” 52(363): 1991–97. 2001.

1024 Skelton, R. P., West, A. G., & Dawson, T. E. “Predicting plant vulnerability to drought in
1025 biodiverse regions using functional traits.” *Proceedings of the National Academy of*
1026 *Sciences*, *112*(18), 5744-5749. 2015.

1027 Sevanto, Sanna, Nate G. Mcdowell, L. Turin Dickman, Robert Pangle, and William T. Pockman.
1028 “How Do Trees Die? A Test of the Hydraulic Failure and Carbon Starvation Hypotheses.”
1029 *Plant, Cell and Environment* 37(1):153–61. 2014.

1030 Sperry, John S. “Evolution of Water Transport and Xylem Structure.” *International Journal of*
1031 *Plant Sciences* 164. 2003.

1032 Teuling, Adriaan J, Remko Uijlenhoet, and Peter A Troch. “Impact of Plant Water Uptake
1033 Strategy on Soil Moisture and Evapotranspiration Dynamics during Drydown.” 33: 3–7.
1034 2006.

1035 Vesala, T., Sevanto, S., Grönholm, T., Salmon, Y., Nikinmaa, E., Hari, P. and Hölttä, T., Effect

of leaf water potential on internal humidity and CO2 dissolution: reverse transpiration and improved water use efficiency under negative pressure. *Frontiers in plant science*, *8*, p.54. 2017.

Westoby, M., Falster, D.S., Moles, A.T., Vesk, P.A. and Wright, I.J., Plant ecological strategies: some leading dimensions of variation between species. *Annual review of ecology and systematics*, *33*(1), pp.125-159. 2002.

Wilkinson, S, and W J Davies. "ABA-Based Chemical Signalling : The Co-Ordination Of." : 195–210. 2002.

Wullschleger, Stan D. et al. "Plant Functional Types in Earth System Models : Past Experiences and Future Directions for Application of Dynamic Vegetation Models in High-Latitude Ecosystems." *Annals of botany* (114): 1–16. 2014.

Yu, Gui-rui, Jie Zhuang, and Keiichi Nakayamma. "Root Water Uptake and Profile Soil Water as Affected by Vertical Root Distribution." *Plant Ecol*: 15–30. 2007.

Zeng, Xubin. "Global Vegetation Root Distribution for Land Modeling." *Journal of Hydrometeorology* 2(5): 525–30. 2001.

## Tables

**Table 1 Parameters used in FATES-Hydro sensitivity analysis**

| Parameters | Biological meaning | Values | Units |
|---|---|---|---|
| $r_a$, $r_b$ | Root distribution: shallow roots vs. deep roots | (0.1, 0.1) – (2 5) | unitless |
| $P50_{gs}$ | Leaf xylem water potential at half stomatal closure stomatal control on safety vs. efficiency | P50x – P20x | Mpa |
| $P50_x$ | Xylem water potential when xylem loss half of the conductance | -3.0[a], -4.8[b] | Mpa |
| $K_{max}$ | Maximum xylem conductivity per unit sap area | 0.88[a], 0.64[b] | kg/MPa/m/s |
| A | Shape parameter of van Genuchten hydrologic function | 0.11855[a], 0.088026[b] | $Mpa^{-1}$ |
| m, n | Shape parameters of van Genuchten hydrologic function | (0.8, 1.25)[a], (0.8, 1.5)[b] | unitless |

a: values for efficient/unsafe xylem
b: values for inefficient/safe xylem

**Table 2. List of major parameters**

| Symbol | Source code name | Value | Units | Description | Source |
|---|---|---|---|---|---|
| $a_{gs}$ | fates_hydr_avuln_gs | 2.5 | unitless | shape parameter for stomatal control of water vapor (slope)exiting leaf | Christoffersen et al., 2016 |
| $\chi$ | fates_hydr_p_taper | 0.333 | unitless | xylem taper exponent | Christoffersen et al., 2016 |
| $\pi_{o,l}$, $\pi_{o,s}$, $\pi_{o,r}$ | fates_hydr_pinot_node | -1.47, -1.23, -1.04 | MPa | osmotic potential at full turgor of leaf, stem, root | Christoffersen et al., 2016 |
| $RWC_{res,l}$, $RWC_{res,s}$, $RWC_{res,r}$ | fates_hydr_resid_node | 0.25, 0.325, 0.15 | proportion | residual fraction of leaf, stem, root | Christoffersen et al., 2016 |
| $\Theta_{sat,x}$ | fates_hydr_thetas_node | 0.65 | $cm^3/cm^3$ | saturated water content of xylem | Christoffersen et al., 2016 |
| $SLA_{max}$ | fates_leaf_slamax | 0.01 | $m^2/gC$ | Maximum Specific Leaf Area (SLA) | TRY |
| $SLA_{top}$ | fates_leaf_slatop | 0.01 | $m^2/gC$ | Specific Leaf Area (SLA) at top of canopy, projected area basis | TRY |
| $V_{cmax,25,\ top}$ | fates_leaf_vcmax25top | 55 | umol $CO2/m^2/s$ | maximum carboxylation rate of Rub. at 25C, canopy top | TRY |
| $b_{opt}$ | fates_bbopt_c3 | 10000 | umol $H2O/m^2/s$ | Ball-Berry minimum leaf stomatal conductance for C3 plants | Calibrated |

## Figures

Figure 1

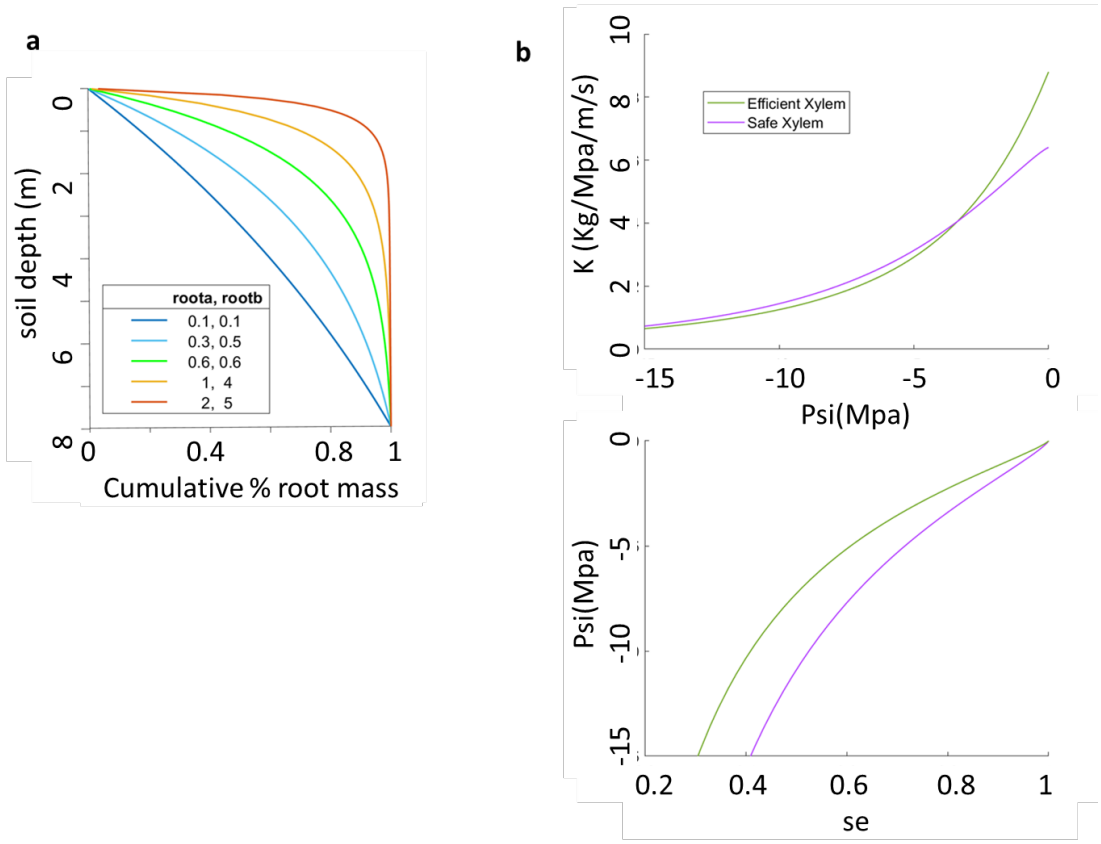


Figure 1. Sensitivity analysis set up for: a) root parameters that give five root distribution scenarios with effective rooting depths of 1m, 3m, 5m, 6.5m, and 8m , and b) two xylem scenarios for safe xylem (P50x=-4.8, Kmax=0.64), and efficient xylem (P50x=-2.5, Kmax=0.88).

1072 Figure 2

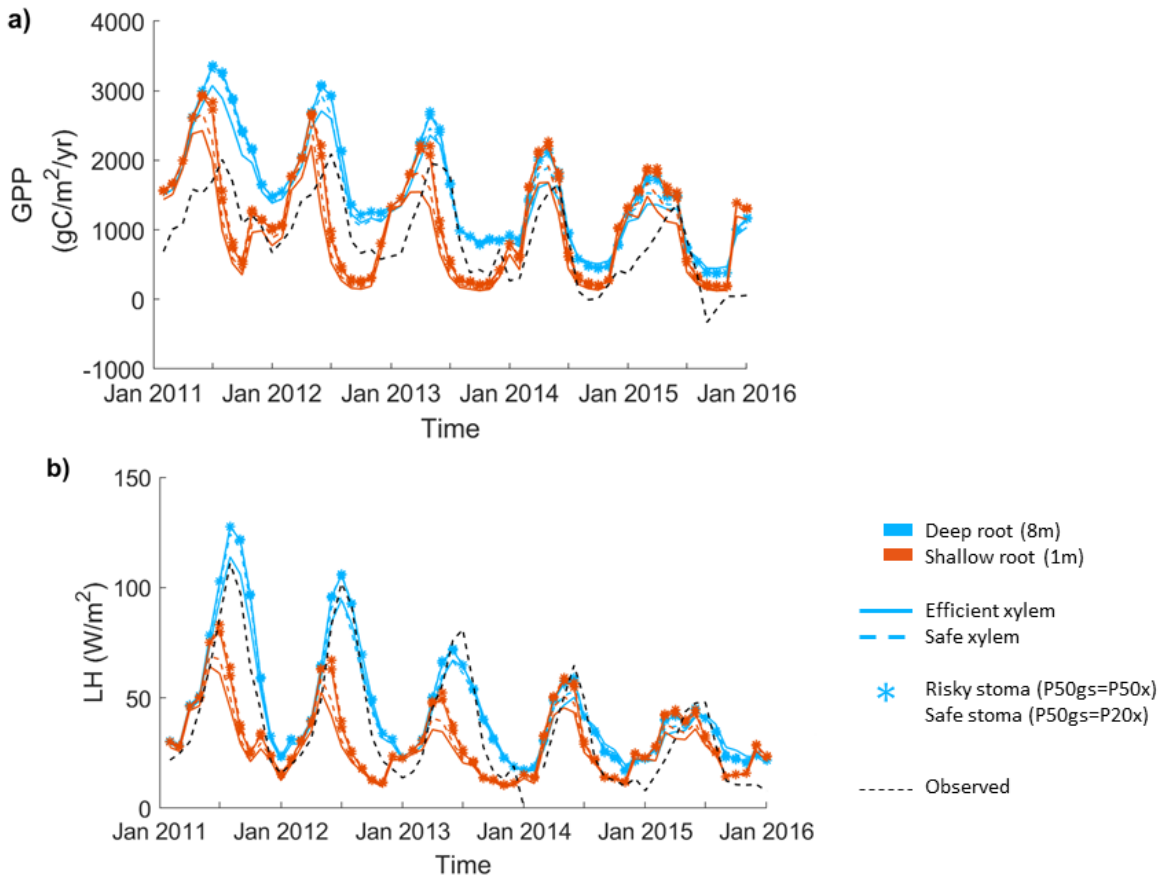


1073

1074 Figure 2. Impact of hydraulic strategies on ecosystem water and energy fluxes: a) monthly mean
1075 gross primary productivity, and B) monthly mean latent heat flux, of the end member cases.

1076

1077

1078 Figure 3

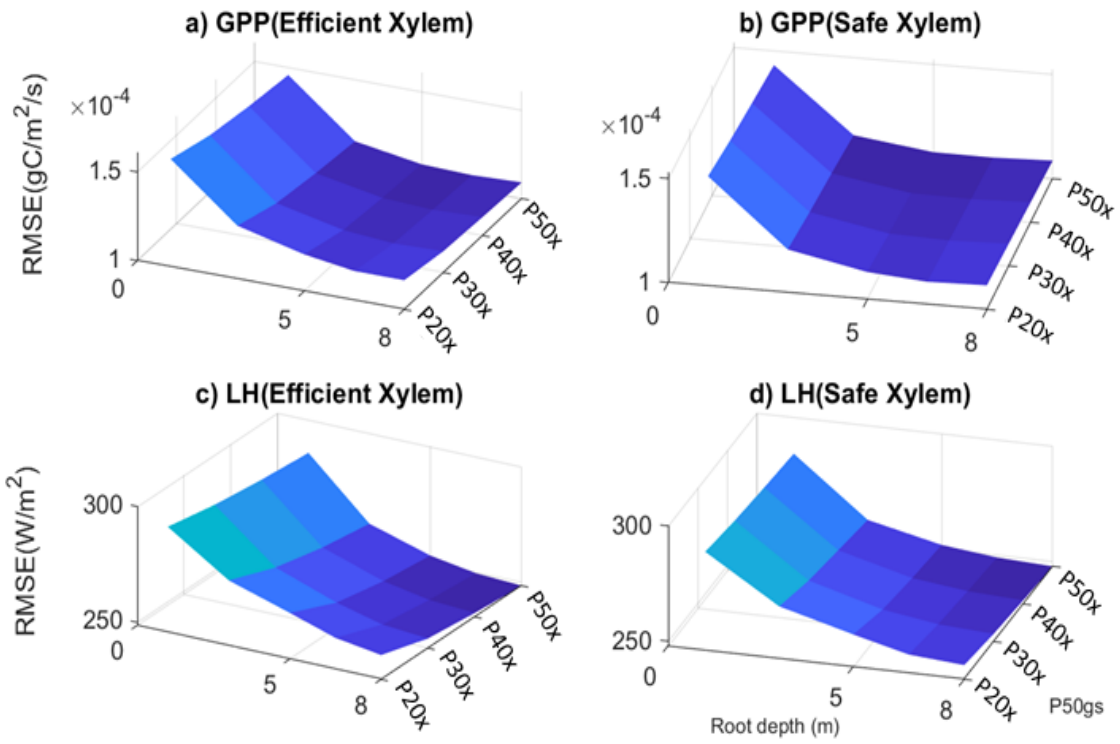


1079

1080 Figure 3. Root mean square error of GPP (a-b), and latent heat flux (c-d) with respect to variation
1081 in input parameters.

1082

1083

1084 Figure 4

1085

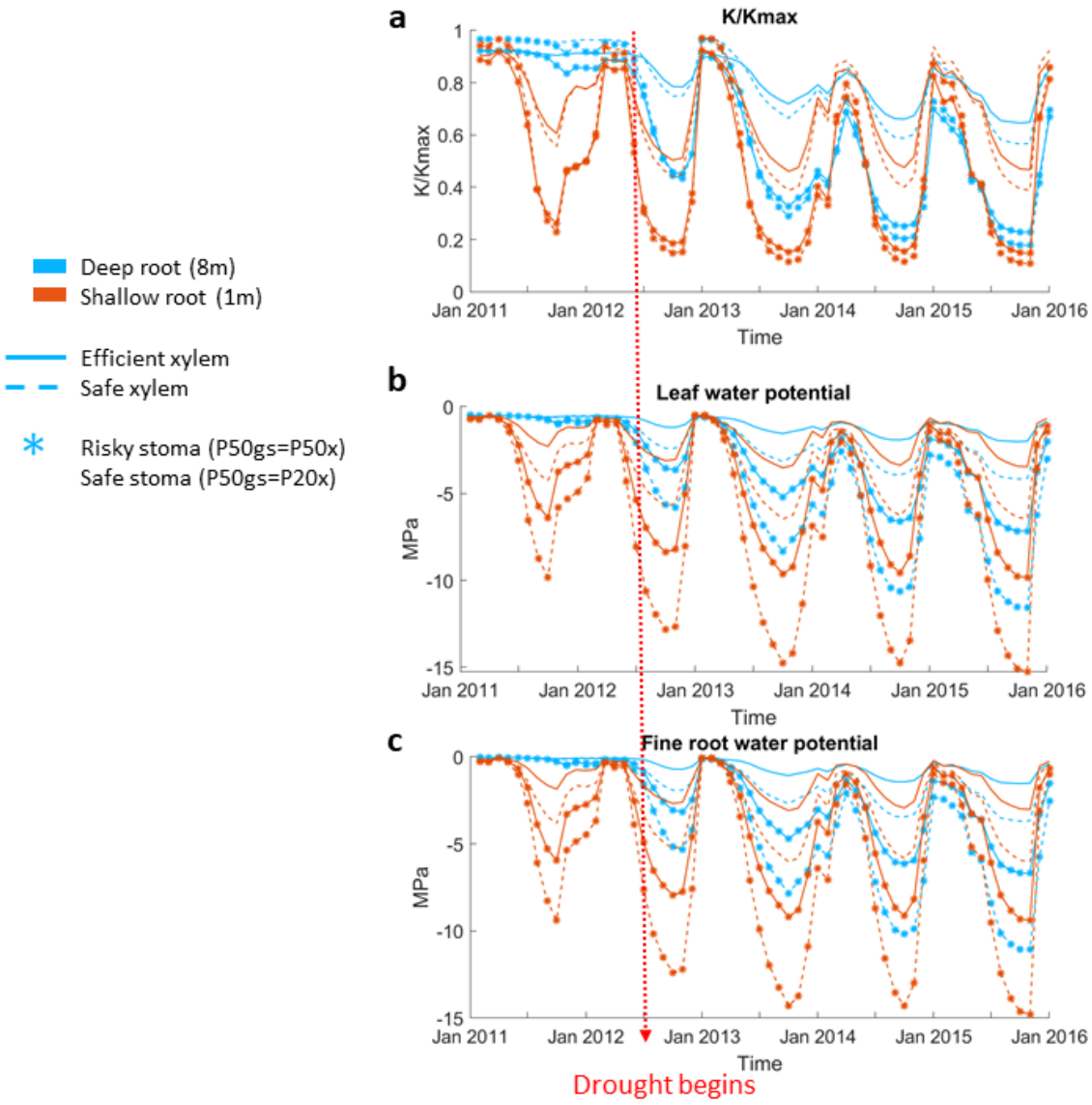


1086

1087 Figure 4. Seasonal and inter-annual variation of plant physiologic characteristics: a) monthly
1088 mean stem fraction of conductance $K/K_{max}$ (a), monthly mean leaf water potential, and c)
1089 monthly mean overall absorbing roots water potential, of the 55cm DBH cohort throughout the
1090 2011-2015 period.

1091

1092

Figure 5

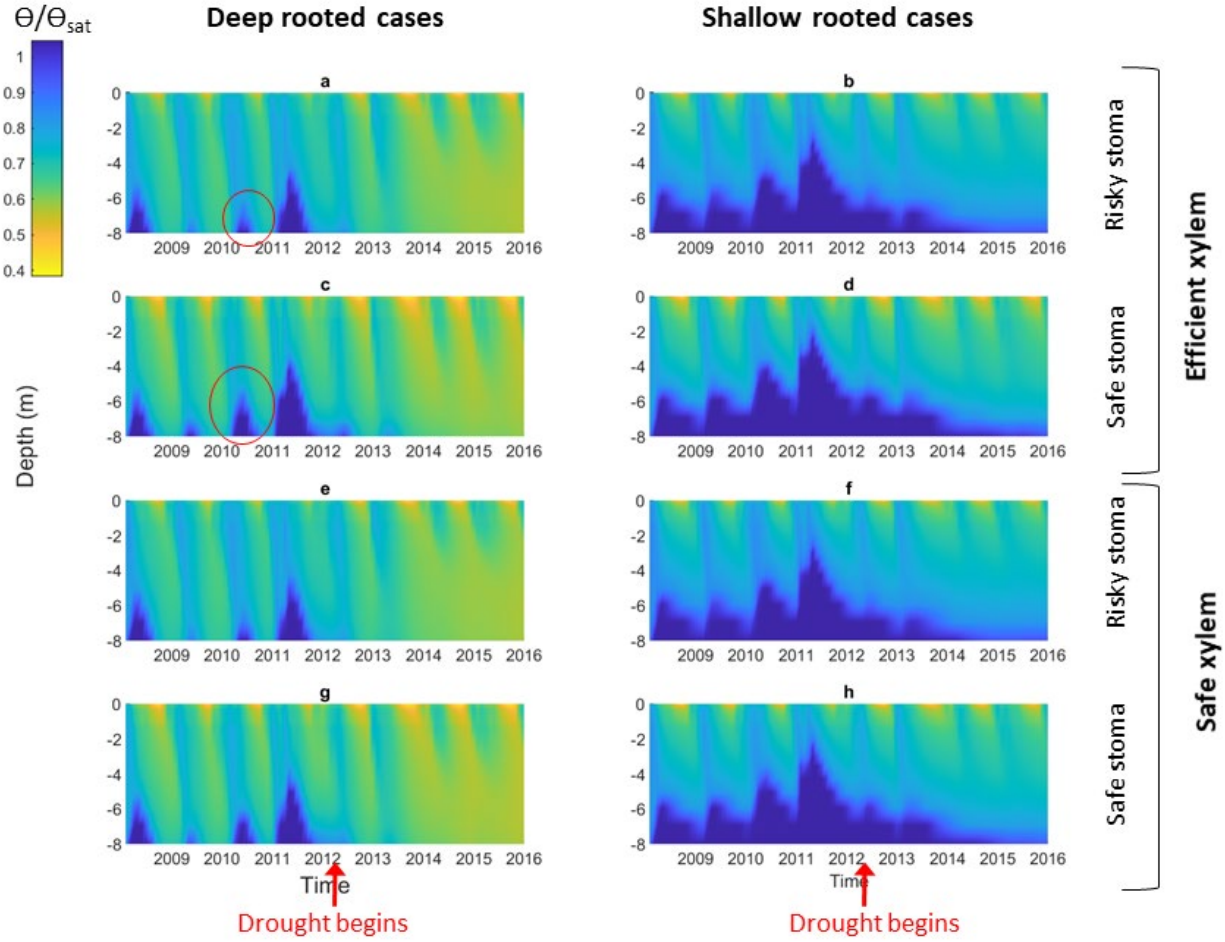


Figure 5. Impact of different combination of rooting depth, xylem and stomatal traits on soil moisture; left column shows deep rooted cases with a) efficient xylem and risky stoma, c) efficient xylem and safe stoma, e) safe xylem and risky stoma, g) safe xylem and safe stoma. Right column shows shallow rooted cases with b) efficient xylem and risky stoma, d) efficient xylem and safe stoma, f) safe xylem and risky stoma, h) safe xylem and safe stoma; red cycle highlights the effect of stomatal traits on deep water storage during the wet season of the pre-drought period

1104 Figure 6

1105

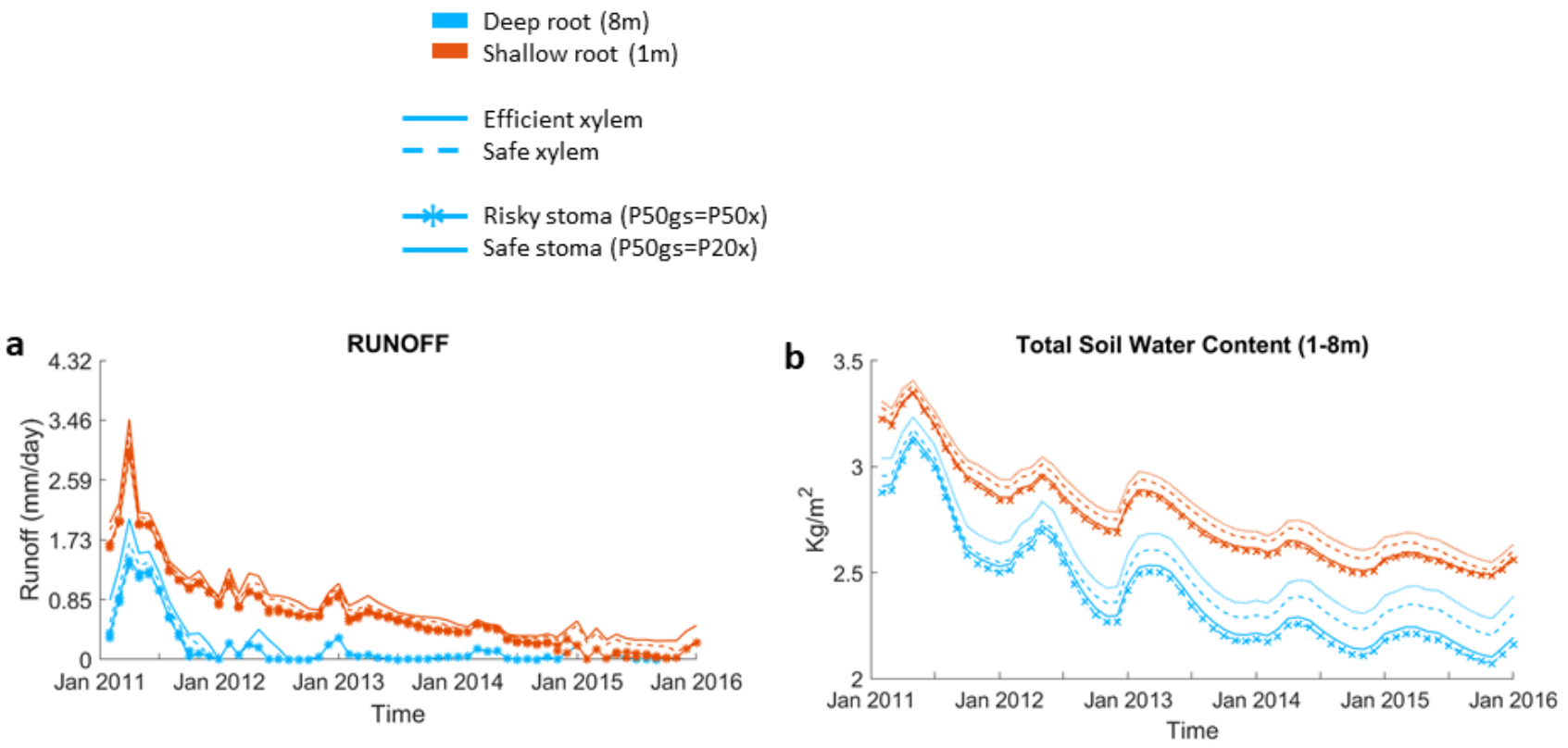


1106

1107 Figure 6. Impact on hydrologic processes: a) mean monthly total runoff, and b) monthly mean total soil water content of the entire soil
1108 column.

Figure 7

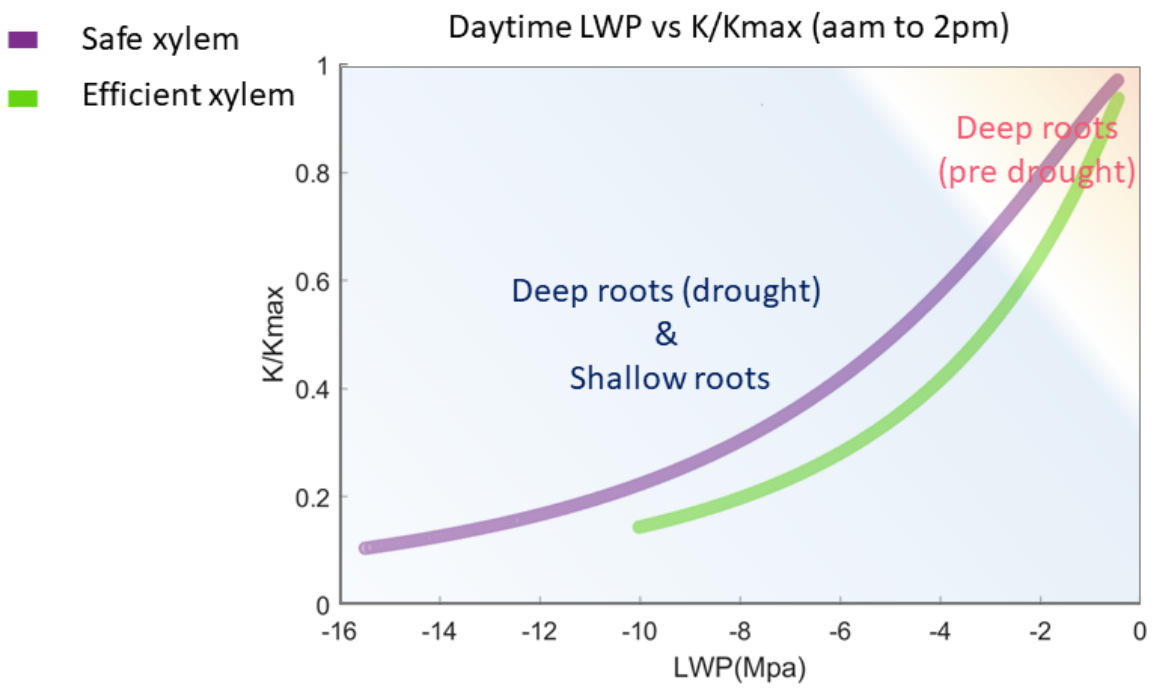


Figure 7. Simulated leaf water potential and fraction loss of conductivity (K/Kmax) of all the cases, which follow the two vulnerability curves.

1115 Figure 8

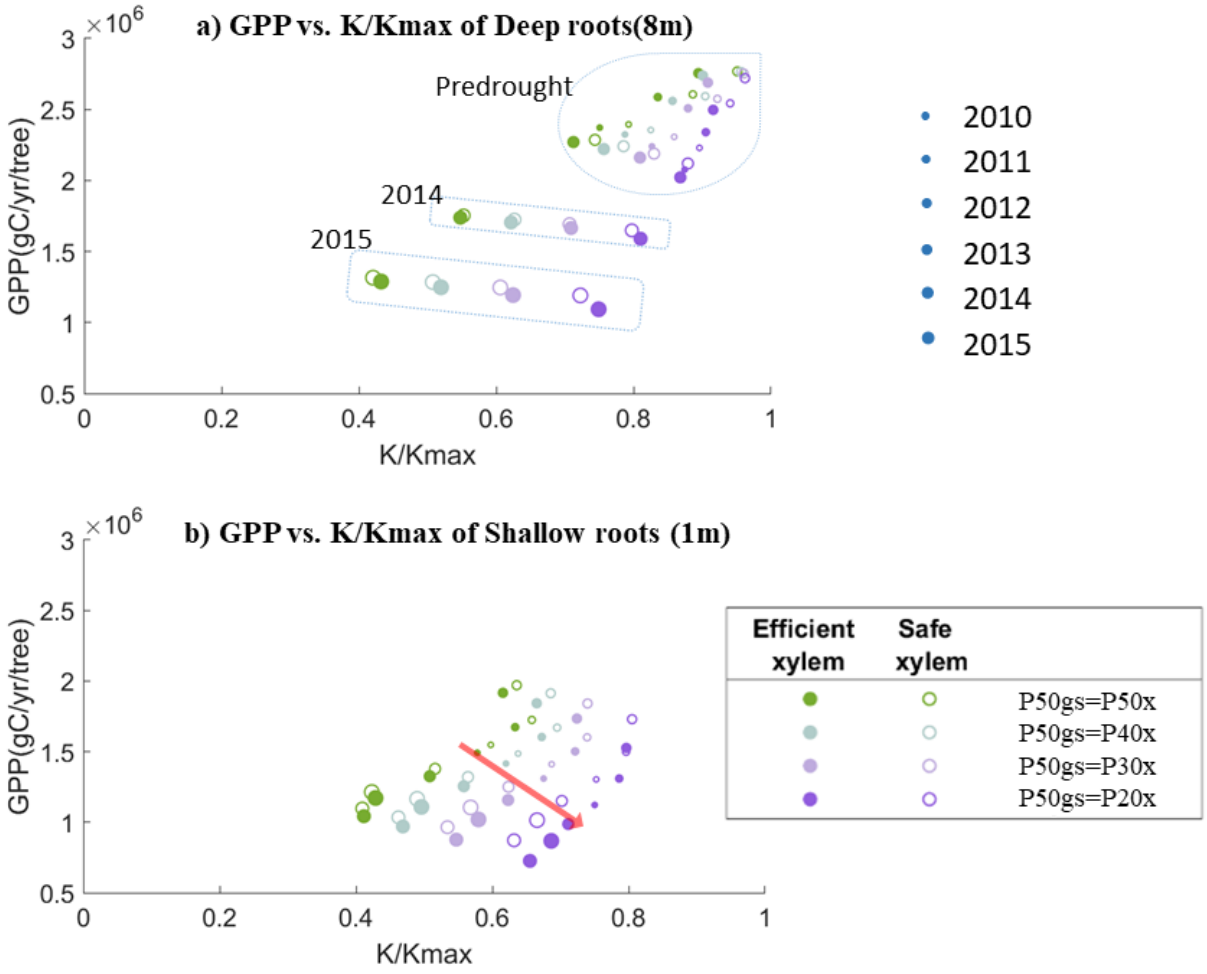


1116

1117 Figure 8. Simulated average annual GPP and fraction of conductance of a 55cm DBH cohort
1118 with a) deep roots (effective rooting depth= 8m) and b) shallow roots (effective rooting depth=
1119 1m).

1120